WETTABILITY BEHAVIOUR OF 3D PRINTED MEMBRANE FOR OIL REMEDIATION

KHAIRUL SYAZWAN NAIM BIN MOHD RAPI

UNIVERSITI TEKNIKAL MALAYSIA MELAKA

WETTABILITY BEHAVIOUR OF 3D PRINTED MEMBRANE FOR OIL REMEDIATION

KHAIRUL SYAZWAN NAIM BIN MOHD RAPI

This report is submitted
in fulfillment of the requirement for the degree of
Bachelor of Mechanical Engineering

Faculty of Mechanical Technology and Engineering

UNIVERSITI TEKNIKAL MALAYSIA MELAKA

JANUARY 2024

DECLARATION

I declare that this project report entitled “Wettability Behaviour Of 3D Printed Membrane for Oil Remediation” is the result of my own work except as cited in the references.

Signature : .....

Name : KHAIRUL SYAZWAN NAIM BIN MOHD RAPI

Date : 27/1/2024

APPROVAL

I hereby declare that I have read this project report and in my opinion this report is sufficient in terms of scope and quality for the award of the degree of Bachelor of Mechanical Engineering.

Signature : 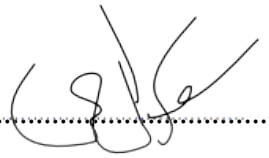

Name of Supervisor : DR. NURUL HILWA BINTI MOHD ZINI

Date : 30/1/2024

DEDICATION

To my beloved mother and father

ABSTRACT

Wettability of a membrane plays an important role in enhancing separation efficiency; it can be assessed by determining the contact angle of liquid on a surface. In recent years, there is a lot of interest in developing hydrophobic surfaces for oil-water separation. However, research on the wettability behaviour of 3 dimensional (3D) printed membranes for oil remediation is not fully explored. The objectives of this study were to characterize the wettability of 3D printed polymer membranes for oil-water separation and to determine the effect of 3D printing process on wettability of polymer membranes. The research methodology involved material preparation, membrane fabrication and coating and material characterization including surface roughness, contact angle measurement and analysis of surface morphology and microporous structure (porosity determination and observation using scanning electron microscopy (SEM)). Results from surface roughness with the higher value is 14.63µm coated membrane for laser power 70Watt and layer thickness 0.12mm bottom surface while the lowest is 8.83µm non-coated membrane 80Watt and 0.06mm. The value for contact angle results of the 3D printed membrane using virgin PA-12 powder (non-coated) of 70Watt and 0.06mm, 70Watt and 0.12mm, 80Watt and 0.06mm, 80Watt and 0.12mm are 138.0°, 149.0°, 137.2°, 139.6° and coated membrane for 70Watt and 0.06mm, 70Watt and 0.12mm, 80Watt and 0.06mm, 80Watt and 0.12mm are 146.0°, 151.9°, 141.4°, 145.3° respectively. Additionally, the analysis of surface morphology and microporous structure using SEM images confirms the presence of a uniform and more porous structure within the coated membrane and for non-coated membrane exhibited more melting and fewer pores. The percentage for porosity results of the 3D printed membrane using virgin PA-12 powder (non-coated) of 70Watt and 0.06mm, 70Watt and 0.12mm, 80Watt and 0.06mm, 80Watt and 0.12mm are 13.83%, 19.44%, 11.88%, 13.78% and coated membrane for 70Watt and 0.06mm, 70Watt and 0.12mm, 80Watt and 0.06mm, 80Watt and 0.12mm are 13.99%, 22.37%, 14.40%, 14.81% respectively. The results demonstrated significant improvements in the surface roughness of the membrane, with the coated membrane showcasing a rougher surface textured that facilitated the creation of air pockets, thus reducing the contact area between the oil and water. Contact angle tests indicated an enhanced oil-repellent property of the coated membrane, as evidenced by higher contact angles, highlighting its capacity to repel oil and encourage water permeation. Moreover, the analysis of surface morphology and microporous structure, conducted through SEM images, confirmed the presence of a uniform and well-defined porous structure within the coated membrane. This structure played a crucial role in enabling the selective passage of water while effectively blocking the passage of oil droplets, thereby ensuring efficient oil-water separation. Porosity tests demonstrated that the membrane maintained its desired porosity, ensuring an efficient flow of fluids while preserving separation effectiveness. The findings concluded that wettability of 3D printed polymer membranes is significantly influenced by specific printing parameters, coatings and roughness specimens. Additional experiments are needed to better comprehend the impact of 3D printing on the switchable wettability of the polymer membrane.

ABSTRAK

Kebolehbasahan membran memainkan peranan penting dalam meningkatkan kecekapan pemisahan; ia boleh dinilai dengan menentukan sudut sentuhan cecair pada permukaan. Dalam beberapa tahun kebelakangan ini, terdapat banyak minat dalam membangunkan permukaan hidrofobik untuk pemisahan minyak-air. Walau bagaimanapun, penyelidikan tentang tingkah laku kebolehbasahan membran bercetak 3 dimensi (3D) untuk pemulihan minyak tidak diterokai sepenuhnya. Objektif kajian ini adalah untuk mencirikan kebolehbasahan membran polimer cetakan 3D untuk pengasingan minyak-air dan untuk menentukan kesan proses cetakan 3D terhadap kebolehbasahan membran polimer. Metodologi penyelidikan melibatkan penyediaan bahan, fabrikasi membran dan salutan dan pencirian bahan termasuk kekasaran permukaan, pengukuran sudut sentuhan dan analisis morfologi permukaan dan struktur mikroporous (penentuan keliangan dan pemerhatian menggunakan mikroskop elektron pengimbasan (SEM)). Hasil daripada kekasaran permukaan dengan nilai yang lebih tinggi ialah membran bersalut 14.63µm untuk kuasa laser 70Watt dan ketebalan lapisan 0.12mm permukaan bawah manakala yang paling rendah ialah 8.83µm membran tidak bersalut 80Watt dan 0.06mm. Nilai hasil sudut sentuhan membran bercetak 3D menggunakan serbuk PA-12 dara (tidak bersalut) 70Watt dan 0.06mm, 70Watt dan 0.12mm, 80Watt dan 0.06mm, 80Watt dan 0.12mm ialah 138.0°, 149.0.0. °, 139.6° dan membran bersalut untuk 70Watt dan 0.06mm, 70Watt dan 0.12mm, 80Watt dan 0.06mm, 80Watt dan 0.12mm masing-masing ialah 146.0°, 151.9°, 141.4°, 145.3° Di samping itu, analisis morfologi permukaan dan struktur mikroporous menggunakan imej SEM mengesahkan kehadiran struktur seragam dan lebih berliang dalam membran bersalut dan untuk membran tidak bersalut dipamerkan lebih cair dan lebih sedikit liang. Peratusan untuk hasil keliangan membran cetakan 3D menggunakan serbuk PA-12 dara (tidak bersalut) 70Watt dan 0.06mm, 70Watt dan 0.12mm, 80Watt dan 0.06mm, 80Watt dan 0.12mm ialah 13.83%, 19.44% , 13.78% dan membran bersalut untuk 70Watt dan 0.06mm, 70Watt dan 0.12mm, 80Watt dan 0.06mm, 80Watt dan 0.12mm masing-masing ialah 13.99%, 22.37%, 14.40%, 14.81% Hasilnya menunjukkan peningkatan ketara dalam kekasaran permukaan membran, dengan membran bersalut mempamerkan tekstur permukaan yang lebih kasar yang memudahkan penciptaan poket udara, sekali gus mengurangkan kawasan sentuhan antara minyak dan air. Ujian sudut sentuhan menunjukkan sifat penghalau minyak yang dipertingkatkan pada membran bersalut, seperti yang dibuktikan oleh sudut sentuhan yang lebih tinggi, menyerlahkan keupayaannya untuk menangkis minyak dan menggalakkan resapan air. Selain itu, analisis morfologi permukaan dan struktur mikroporous, yang dijalankan melalui imej SEM, mengesahkan kehadiran struktur poros yang seragam dan jelas dalam membran bersalut. Struktur ini memainkan peranan penting dalam membolehkan laluan air terpilih sambil menghalang laluan titisan minyak secara berkesan, dengan itu memastikan pemisahan minyak-air yang cekap. Ujian keliangan menunjukkan bahawa membran mengekalkan keliangan yang diingini, memastikan aliran cecair yang cekap sambil mengekalkan keberkesanan pengasingan. Penemuan menyimpulkan bahawa kebolehbasahan membran polimer cetakan 3D dipengaruhi dengan ketara oleh parameter cetakan tertentu, salutan dan spesimen kekasaran. Eksperimen tambahan diperlukan untuk memahami dengan lebih baik kesan pencetakan 3D pada kebolehbasahan boleh tukar membran polimer.

ACKNOWLEDGEMENT

I would like to take this opportunity to express my sincere gratitude and appreciation to all the individuals who have supported and contributed to the successful completion of my final year project.

First and foremost, I would like to extend my deepest appreciation to my supervisor, Dr Nurul Hilwa Binti Mohd Zini, for their invaluable guidance, expertise and continuous support throughout this project. Their knowledge, dedication and encouragement have been instrumental in shaping the direction and execution of this research. I am grateful for their mentorship and the opportunities they have provided me to enhance my skills and knowledge in this field. I would also like to express my heartfelt gratitude to the master students, Nurul Afiqah Binti Arbain who have generously shared their time, knowledge and expertise with me. Their support and willingness to assist me whenever needed have been invaluable. Their guidance, insightful discussions and practical advice have greatly contributed to the development and improvement of my research work.

I am also thankful to the faculty members and teaching staff for their valuable input, constructive feedback and encouragement throughout my academic journey. Their commitment to excellence and their passion for imparting knowledge have been a constant source of inspiration. I would like to acknowledge the assistance and cooperation of my fellow classmates and friends who have provided support, encouragement and stimulating discussions. Their camaraderie and shared experiences have made this academic journey more enjoyable and memorable.

Furthermore, I would like to express my appreciation to the technical staff and laboratory assistants for their assistance and support during the experimental work. Their expertise, patience and willingness to lend a helping hand have been vital in the successful completion of the practical aspects of this project. To all those mentioned above and to anyone else who has contributed to my growth and development, I am sincerely grateful for your support, encouragement and collaboration. This project would not have been possible without your contributions and I am honoured to have had the opportunity to work with such amazing individuals.

TABLE OF CONTENTS

LIST OF TABLES

LIST OF FIGURES

LIST OF ABBEREVATIONS

ISO	International Organization for Standardization
OCA	Optical Contact Angle
CO_2	Carbon dioxide
MF	Microfiltration
UF	Ultrafiltration
NF	Nanofiltration
RO	Reverse Osmosis
APIs	Active Pharmaceutical Ingredients
AM	Additive Manufacturing
CAD	Computer-Aided Design
SLA	Stereolithography
SLS	Selective Laser Sintering
FDM	Fused Deposition Modelling
UV	Ultraviolet
ILs	Ionic Liquids
PA-12	Polyamide-12
3D	Three Dimensional
LCD	Liquid-crystal display
SEM	Scanning Electron Microscope

LIST OF SYMBOLS

W	=	Weight
°	=	Degree
θ	=	Angle
%	=	Percent
$°C$	=	Celsius
σ	=	Standard Deviation
$\sum$	=	Summation
x_i	=	Individual value
μ	=	Mean average
N	=	Total number of values

CHAPTER 1

INTRODUCTION

1.1 Background

An oil spill is characterized as an unintended release of liquid industrial waste into the environment, caused by human activity. It is a type of pollution that can have catastrophic effects on the ecosystem, leading to significant environmental damage.

Over the past five decades, numerous oil spills have occurred in oceans across the globe (AFP, 2018). These incidents not only put aquatic life and ecosystems at risk, but also pose a danger to human life. The effects of oil spills can be far-reaching, with potential consequences for human health and the economy. Spilled oil can contaminate water supplies, damage natural habitats and harm or kill wildlife (Dhaka and Chattopadhyay, 2021). The resulting damage can also affect local industries, such as fishing, tourism and recreation, leading to significant economic losses for affected communities. If swift action is not taken, the world may face a serious food and environmental crisis. Due to the significant and devastating impacts of oil spill pollution on biodiversity, including health impacts, there has been much criticism of this issue in the past two decades (Ritchie, 2022).

In 1992, a collision between an oil tanker and a ship in the Malacca Straits led to a devastating oil spill, as depicted in Figure 1.1. The collision caused the release of approximately 12,000 tonnes of crude oil into the surrounding waters. Oil spills have long been recognized as one of the most significant environmental issues associated

with the oil and gas industry, as they can lead to extensive shoreline contamination (Energy, 2021).

Figure 1.1: Oil spill pollution in Strait Malacca. (Source: rivieramm.news)

The clean-up efforts required to mitigate the damage caused by an oil spill can be extensive and costly, requiring specialized equipment and expertise. Oil spill prevention is also difficult, however there are several ways are usually use to oil spill remediation in these situations (Agarwal, 2021). In this instance, bio inspired oil which is oil remediation techniques can be used to remove oil contaminants from both immiscible oil–water mixtures (Bhushan, 2019). Membrane separation techniques have recently been developed and are thought to be an excellent method for separating oil from water, particularly small droplet-containing wastes (Barambu *et al.*, 2021). Furthermore, the membrane technology is low-cost and simple to use (Sutrisna *et al.*, 2022). The fabrication of membranes has utilized three-dimensional (3D) printing, providing the benefit of creating intricate structures and assembling them in a single-step process, a departure from conventional manufacturing techniques. Research highlighted the successful creation of 3D-printed microfiltration membranes through selective laser sintering with semi-crystalline polyamide, emphasizing the influence of

sintering process parameters on the membrane's structure and performance (Yuan *et al.*, 2017).

1.2 Problem Statement

Polymer membranes, produced through 3D printing, demonstrated the ability to modify their wettability, showcasing hydrophobic characteristics when exposed to water in standard atmospheric conditions (Yuan *et al.*, 2020). This characteristic enables these printed membranes to be effectively utilized in oil spill remediation. However, due to the significant impact of 3D printing on wettability, variations in 3D printing parameters specimen may compromise the superhydrophobicity of the printed polymer membrane.

Therefore, further experimental investigations are necessary to gain a better understanding of the effect 3D printing switchable wettability of the printed polymer membrane.

1.3 Objective

The objectives of this project are as follows:

1. To characterize wettability of 3D printed polymer membranes for oil-water separation.
2. To determine the effect of 3D printing process on wettability of polymer membranes.

1.4 Scope of Project

The scopes of this project are:

1. Specimens made from virgin polyamide powder were fabricated using Selective Laser Sintering (SLS) by setting the laser power 70 and 80 Watt with the slice or layer thickness set at 0.06 and 0.12mm.
2. The surface morphology, porosity, contact angle measurement and surface roughness (in accordance with ISO 4287:1997) of the specimens with different 3D printing parameters were assessed.
3. Experiments were conducted in dry environmental conditions. The set-up for the dry conditions was maintained between 25°C to 27°C.
4. Paraffin candle was used to coat the 3D printed specimens.

CHAPTER 2

LITERATURE REVIEW

2.1 Oil Spill Pollution

Oil is used as an energy source in a wide range of industrial applications all over the world. Oil contains a wide spectrum of basic components that can be used to make monomers and composites (Dhaka and Chattopadhyay, 2021). The transportation industry has resulted in a large amount of used oil as a source of power and such fuels continue to affect the environment.

Figure 2.1 depicts the world's greatest oil spill in the Gulf of Mexico in 2010. Over the span of 85 days, literally thousand tonnes of fuel moved over the oceans, damaging aquatic ecosystems (Wolok *et al.*, 2020).

Figure 2.1: Shell spills 88,200 gallons of oil into Gulf of Mexico. (Source: https://news.mongabay.com).

Due to mechanical disturbance, transportation, equipment and a lack of tank monitoring, oil contamination disasters are unavoidable (Wolok *et al.*, 2020). The massive amount of petrol floating on the ocean surface, which covers the surrounding

flora and wildlife as well as the shoreline environs, can be considered the spill's initial harmful impact on pelagic ecology. Apart from creating a terrible aesthetic environment, it has a significant impact on marine ecology, resulting in the loss of many marine and littoral creatures. Pelagic pollution modifies the morphological, biochemical and biotic characteristics of seas and littoral regions, hurting species and habitat and lowering the ecological production efficiency of pelagic populations (Cantonati *et al.*, 2020) .

Accidents related to tankers, barges, pipelines, refineries, drilling rigs and storage facilities are the most prevalent sources of oil spills. Human error or negligence, technical flaws, natural calamities such as storms, terrorist activities, military conflicts, thieves, or illegal oil dumps can all result in spills (NOAA, 2021).

From 1970 to 2020, 50% of large spills happened when ships were located at sea because of collisions, accidents when anchoring, with collisions, accidents and grounding accounting for 58% of the causes (Sackeyfio, 2021). Figure 2.2 shows that when the ships were limited to land or confined seas, these same characteristics accounted for an even higher percentage of spills at 9%.

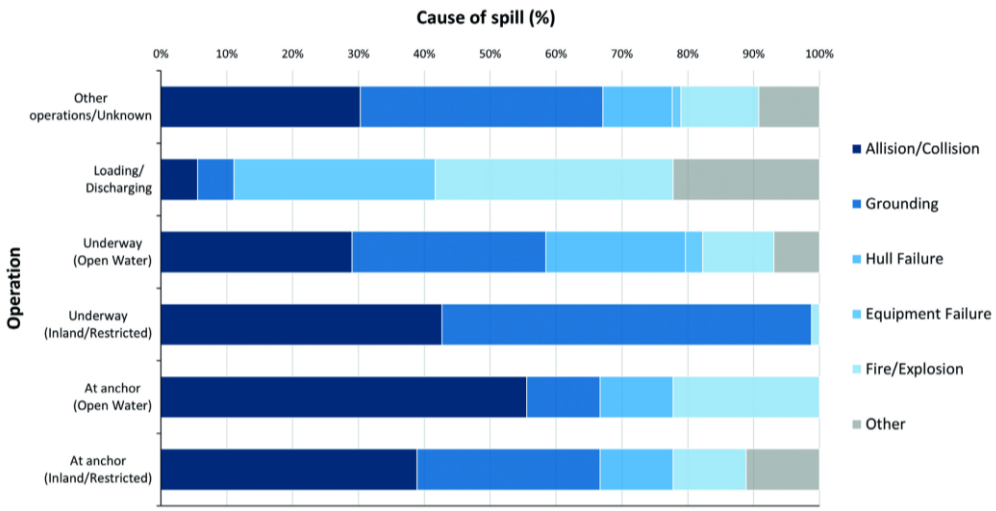

Figure 2.2: Incidence of large spills (more than 700 tonnes) by operation at time of incident and primary cause of spill, 1970-2020. (Source: itopf.org)

2.1.1 Oil Spills Clearance Methods

Oil spills and slicks clearing is one of the most controversial topics since it is impossible to clean up all the oil that has been discharged and spilled into the ocean (Wolok *et al.*, 2020). There are four categories of oil spill clean-up: physical methods, chemical methods, thermal or in-situ burning methods and bio remediation.

1. Physical Methods

Physical measures are commonly used to restrict and control the spread of oil after a spill while keeping the fluid's chemical properties (Dhaka and Chattopadhyay, 2021). There are many examples of physical methods to clean oil spill such as booms, skimmers and adsorbent materials.

a. Booms

Boom is a common tool used to control the spread of oil spills and slicks. Aside from boom construction, tides, air movement and speed all have a big impact on how well booms work (Dhaka and Chattopadhyay, 2021). Figure 2.3 displays the many sorts of booms.

Figure 2.3: Boom types: a) Fence booms b) Curtain booms c) Resistant booms of fire (Source: Anh Tuan Hoang et al., 2018).

Fence booms are suspended structures constructed of stiff or semi-stiff material. It is used to prevent oil from flowing, with around 60% of the fence boom immersed in water (Dhaka and Chattopadhyay, 2021). Meanwhile, curtain booms are large circular foam-filled chambers that float on the water's surface. They are impermeable yet absorbent platforms. Polyurethane, polystyrene and bubble wrap are frequently used in its construction. Lastly, the fireproof materials are utilized to make fire-resistant booms. Fire-resistant booms are dependable and have a high potential for decreasing the negative impact of a fire occurrence caused by an oil leak or an oil slick in the saltwater layer (Pete, Bharti and Benton, 2021). The disadvantages of fire-resistant booms include their high cost and difficulty in transporting due to their heavyweight and size.

b. Skimmers

Skimmer equipment is used in conjunction with booms to recover oil spills and slick off the seawater's surface after utilizing booms to limit the effective area of an oil leak (Pete, Bharti and Benton, 2021). Salvage oil can be reused because the oil characteristics are conserved. Skimmers have the advantage of being automatically drawn from the coast and hauled by ships. Figure 2.4 depicts the skimmers.

Figure 2.4: Skimmers. (Source: oilspillprevention.org)

c. Adsorbent materials

Adsorbent materials are considered experts in cleaning oil spills in the final clean-up phase after the use of maximum oil and water-repellent skimmers. Adsorbent materials are classified into three types: natural organic materials, inorganic sorbent materials and synthetic materials (Dhaka and Chattopadhyay, 2021). To absorb and collect oil, the sorbent substance is injected into the oil slick (Duman, Diker and Tunç, 2021).

Figure 2.5: Adsorbent materials. (Source: Hammouda, 2021)

2. Chemical Methods

Chemical methods for cleaning up oil spills involve the use of various chemicals to address the challenges posed by spilled oil. These methods aim to enhance the natural processes of oil degradation, improve recovery efficiency, or contain and mitigate the impact of the spill. There are two chemical methods known as dispersants and solidifiers which change the properties of oil.

a. Dispersants

Surfactant-containing dispersants can be used in large regions. When sprayed onto the oil, surfactants solutes reduced the contacting surfaces tension between oil and water (Hoang, 2018). Oil dispersion and bio degradation in water are helped by

this. Dispersants are good at cleaning up 90% of oil spills quickly in stormy seas, reducing emulsification and accelerating natural decomposition. However, drawbacks include the use of hazardous substances, inefficiency in calm waters, challenges with thin oil slicks due to easy losses and high costs (Pete, Bharti and Benton, 2021). The dispersants employed in an oil spill are depicted in Figure 2.6.

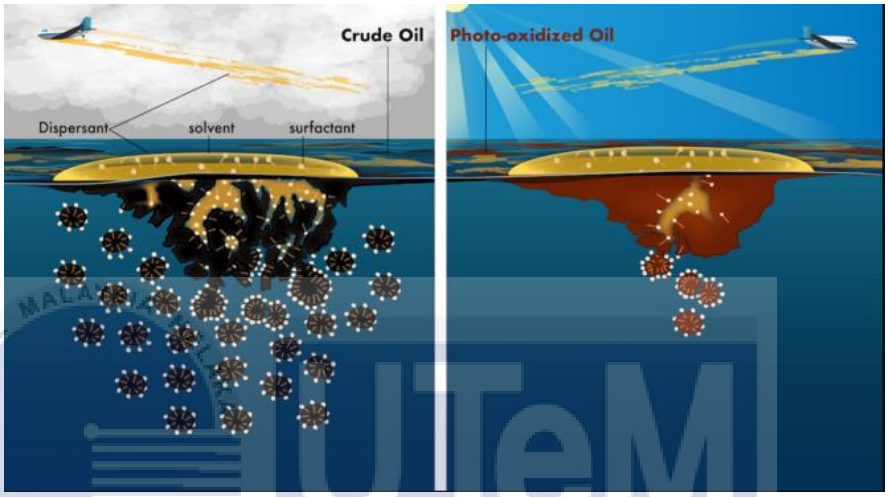

Figure 2.6: Dispersants. (Source: Phys.org)

b. Solidifiers

Solidifiers are dry granular substances that react with oil components to convert liquid oil into a solid state that may be easily removed. Solidifiers are used in booms, pillows and pads to turn oil spills into solid or semi-solid materials (Hoang, 2018). Although the efficacy of solidifiers is reliant on the nature and composition of the oil spill and slick, solidifiers have the advantage of being able to be used in rough seas. Solidifiers have not previously been employed because they are less efficient than dispersants (Motta, Stoyanov and Soares, 2018). The solidifiers are depicted in Figure 2.7.

Figure 2.7: Solidifiers (Motta, 2018)

3. Thermal or in-situ burning method.

Thermal or in-situ burning method is used to mitigate the hazards and repercussions of an oil slick and spill on the in-water ecosystem and the marine environment (Hoang, 2018). According to (Hoang, 2018), thermal or in-situ burning technologies have the potential to eliminate 100-300 tonnes of oil spill and slick each hour. Heliport equipment, a flamethrower draped beneath the helicopter, or an oiled cloth saturated in diesel fuel are utilized to ignite. This strategy, however, is only effective if the oil slick on the water is large enough to burn a large amount of oil at once, the oil slick is thick enough to continue combustion, the seawater is calm and the oil slick is located far enough away from sensitive zones, facilities and equipment (Dhaka and Chattopadhyay, 2021). Because of its capacity to sustain conditions favourable to combustion for an extended period when utilized in ice, cold water, or snow, in-situ burning improved its value in oil spill clean-up (Agarwal, 2021). Although this approach is effective at limiting the oil leak, it has various downsides, the most notable of which being the danger of secondary flames spreading. Figure 2.8 depicts the in-situ burning procedure.

Figure 2.8: In-situ burning procedure. (Source: safetymanagement.eku.edu)

4. Bio remediation

Bio remediation defined as normal cycle in which complex chemicals and molecules are degraded, broken down and metabolized by microbes in attempt to recover as well as maintain environmental balance. Bio remediation is a technique used to aid in the cleanup of oil spills by adding a variety of different beneficial bacteria to speed up the normal bio degradation process. It will aid in protecting afflicted areas from the dangers of an oil spill and preventing future environmental damage (Pete, Bharti and Benton, 2021). The bio degradation process will take 2 to 4 weeks if the oil spill has a high concentration (Dhaka and Chattopadhyay, 2021). Throughout the bio degradation phase, microorganisms must acclimatize to the marine environment for at least a week and the entire bio remediation process can take months, if not years (Pete, Bharti and Benton, 2021). In all meteorological conditions, the bio degradation process is suitable. It's quick and cheap and the product just contains CO_2 and water after biodegradation. Even though no oil is produced, the wastes are continuously metabolized by a wide range of microorganisms. Bio remediation method depicted in Figure 2.9.

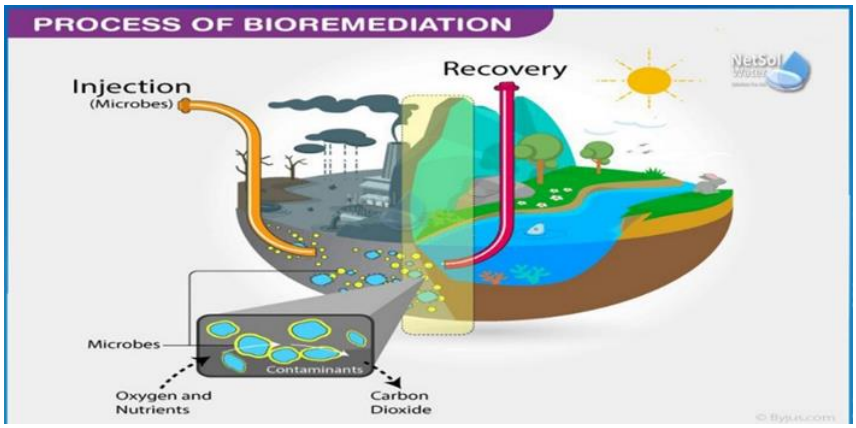

Figure 2.9: Bio remediation method. (Source: https://byjus.com/biology/bioremediation/)

Numerous physical and chemical methods have been developed using various concepts for destabilizing oil-water emulsion for easy separation of oil from water. However, these methods have several drawbacks, including low separation efficiency, high costs, complex operation (in certain cases) and most importantly some methods produce secondary pollutants and are ineffective when it comes to separating emulsions with droplet sizes smaller than 10 mm. Thus, for ongoing industrial development and environmental sustainability, it is imperative to develop sustainable, dependable and efficient technology with a small environmental footprint. Technology that is based on membranes has become a viable alternative. The technology is developing quickly and is anticipated to overtake other methods as the primary means of treating oily wastewater soon (Barambu *et al.*, 2021).

2.2 Membrane

Membranes are used in a variety of applications, ranging from water treatment and industrial processes to healthcare and energy production. These thin, selective barriers have transformed separation and filtering procedures by allowing for efficient and precise control of the passage of substances based on their properties (Ye, 2023). Membranes have become vital instruments in a variety of sectors, providing purification, concentration and separation solutions. Figure 2.10 depicts the 3D printed membrane.

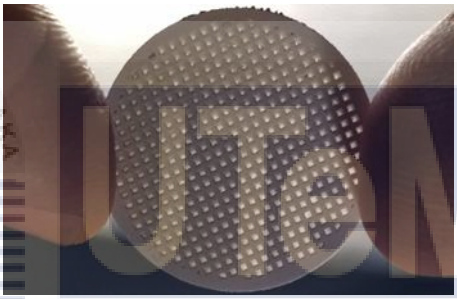

Figure 2.10: 3D printed membrane. (Source: Runice3Dprinted.org)

Membranes are based on the essential need to separate various components or substances from mixtures. Traditional procedures frequently involve complicated and energy-intensive operations like distillation or evaporation (Ye, 2023). Membranes, on the other hand, provide a more sustainable and cost-effective solution by selectively allowing certain molecules or particles to flow through while keeping others (Xu et al. 2021).

A membrane is a physical barrier that is designed to have specific properties that allow substances to be separated based on their size, charge, solubility, or other molecular features (Lazarenko et al. 2022). These qualities can be adjusted by using the right materials and manufacturing procedures. Membranes can be manufactured

from a variety of materials, including polymers, ceramics, metals and composites, each having its own set of benefits and drawbacks (Xu et al. 2021).

Membranes' versatility comes from their capacity to meet a variety of separation criteria. Membranes can be constructed to conduct microfiltration, ultrafiltration, nanofiltration, or reverse osmosis depending on the application (Ezugbe and Rathilal, 2020). These membranes are differentiated by their pore diameters and separation methods, which enable precise control over the passage of particles, molecules, or liquids (Ye, 2023).

Energy efficiency of membranes is one of their primary advantages. Unlike classic separation processes, which frequently require high temperatures, membranes can work at ambient or moderate temperatures, considerably lowering energy use (Xu et al. 2021). Furthermore, membranes have compact and modular designs that make them easily scalable and adaptable to a variety of process requirements (Ye, 2023). Because of their selective nature and precise separation capabilities, they produce higher-quality products, decrease waste and increase process efficiency.

Membrane technology has several applications in a wide range of industries. Membranes are utilized in the water sector to address worldwide water scarcity and environmental concerns by desalination, water purification and wastewater treatment (Lazarenko et al. 2022). Membranes are also important in the pharmaceutical and biotechnology industries, enabling medication purification, protein separation and impurity elimination. Furthermore, membranes are employed in gas separation, food and beverage processing, chemical production and a variety of other applications requiring accurate separation and filtration.

In conclusion, membranes have revolutionized separation and filtration processes by providing efficient, long-term and accurate control over the flow of

substances. Their versatility, energy economy and wide range of uses have made them vital instruments in a variety of sectors. Membranes are predicted to play a growing role in tackling global concerns such as clean water, healthcare and sustainable development as technology advances.

2.2.1 Type of Membrane

There are many types of membranes that can be used for oil-water separation such as microfiltration, ultrafiltration, nanofiltration and reverse osmosis. Figure 2.11 depicts the type of membrane.

I. Microfiltration Membranes

Microfiltration membranes (MF) contain pores that are relatively big, often ranging from 0.1 to 10 µm (Larsen, 2022). To remove suspended sediments, germs and big particles, they typically use a size exclusion method. Water treatment uses MF membranes to remove impurities from drinking water, wastewater and industrial effluents. They are also utilized in the food and beverage industries for clarification operations such as particle removal from juices and dairy products (Larsen, 2022).

II. Ultrafiltration Membranes

Ultrafiltration membranes (UF) feature lower pore diameters than MF membranes, typically ranging from 0.1 µm to 0.01 µm (Larsen, 2022). They are effective at separating macromolecules, viruses, proteins and colloids. UF membranes work by size exclusion, making them ideal for protein purification, concentration and fractionation operations in the biotechnology and pharmaceutical industries. Furthermore, UF membranes are utilized in water treatment to eliminate germs and

viruses, as well as in dairy processing for protein separation and whey fractionation (Larsen, 2022).

III. Nanofiltration Membranes

Nanofiltration membranes (NF) contain pores that are significantly smaller, typically ranging from 0.01 µm to 0.001 µm. They use size exclusion and charge interactions to remove divalent ions, organic debris, colorants and insecticides selectively. NF membranes are used in a variety of applications, including water softening, colour removal in textile industries and dye solution purification (Lazarenko et al. 2022). They are also used in the pharmaceutical industry to separate and purify active pharmaceutical ingredients (APIs).

IV. Reverse Osmosis Membranes

Reverse osmosis membranes (RO) have the smallest pore diameters, which are often less than 0.001 µm. They use both size exclusion and a solute concentration gradient to remove dissolved salts and pollutants from water (Ezugbe and Rathilal, 2020). RO membranes are widely employed in desalination procedures to produce fresh water from seawater or brackish water sources. They are also used in water purification systems, such as the elimination of pollutants in drinking water production.

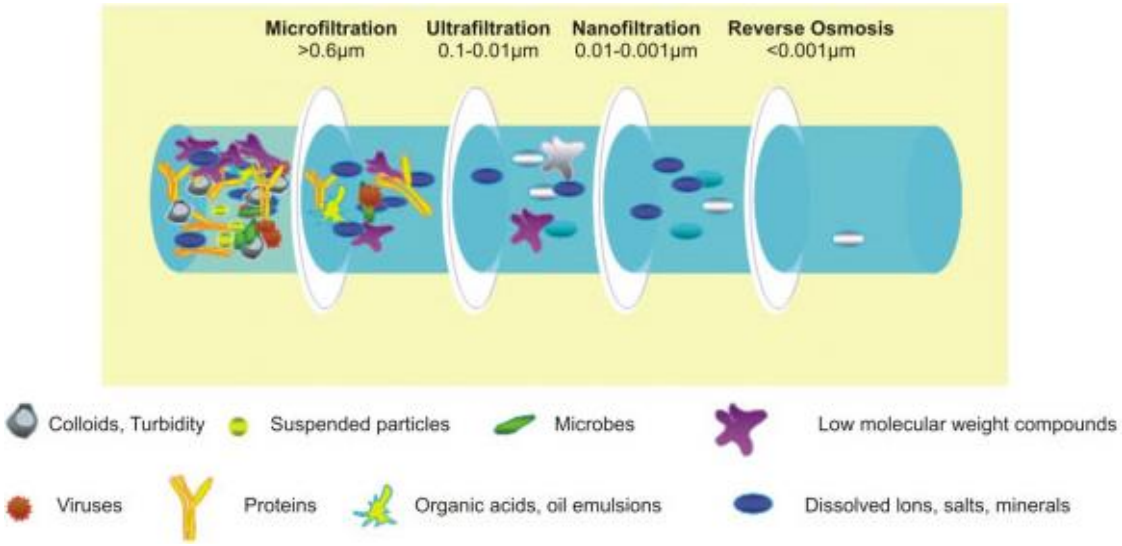

Figure 2.11: Type of membrane. (Source: http://surl.li/ovfmh)

2.2.2 Application Membrane Process

Membrane processes are a class of separation procedures that employ membranes to selectively separate or concentrate certain components from a mixture. These processes entail the use of membranes as barriers to allow certain substances to pass while retaining or rejecting others based on their qualities. Membrane processes have grown in relevance in a variety of industries due to its efficiency, adaptability and environmental friendliness. Here are a few examples of commonly utilised membrane processes:

I. Filtration

Filtration is the most fundamental and commonly utilised membrane process. It entails passing a fluid or gas over a membrane to separate suspended solids, particles, or microbes from the liquid or gas stream (Xu et al. 2021). Filtration procedures, such as microfiltration and ultrafiltration, are widely employed in water and wastewater treatment, air purification and food processing (Larsen, 2022).

II. Ultrafiltration (UF)

Ultrafiltration is a membrane process with a lower cut-off molecular weight than nanofiltration. It's utilised to separate macromolecules, proteins, colloids and suspended particles from liquids (Larsen, 2022). UF is frequently used in the dairy business for protein concentration and fractionation, as well as in the biopharmaceutical industry for therapeutic protein purification.

III. Nanofiltration (NF)

Nanofiltration is a membrane process that combines reverse osmosis and ultrafiltration (Lazarenko et al. 2022). It works at lower pressures than RO and may selectively separate divalent ions, organic materials and some tiny molecules while preserving monovalent ions and solvent molecules. In the pharmaceutical and culinary industries, NF is often employed in water softening, colour removal and the separation of specific components (Xu et al. 2021).

IV. Reverse Osmosis (RO)

Reverse osmosis is a membrane process that is used for water desalination and purification. It entails applying pressure to overcome osmotic pressure and drive water molecules through a semi-permeable barrier, leaving dissolved salts and other contaminants behind (Ezugbe, 2020). RO is commonly employed in saltwater desalination, brackish water treatment and high-quality drinking water production.

These membrane processes have various advantages, including energy efficiency, small system design, easy scalability and environmental friendliness. They are used in a variety of industries, including water treatment, medicines, food and beverage processing, chemical processing and energy generation. Continued research

and development in membrane technology is likely to promote significant breakthroughs in membrane processes, resulting in greater separation efficiency, lower prices and expanded applications in the future.

2.2.3 Membrane Fabrication

There are two types of membrane fabrication:

1) Chemical membrane

The production of chemical membranes, formed through intricate processes like solution casting and phase inversion involving polymers and solvents, offer a versatile solution for various separation needs. These complex birthrights imbue them with a potent arsenal: a vast range of pore sizes and selectivity, tailorable to the most specific separation needs (Koros, 2014). From filtering delicate pharmaceutical solutions to scrubbing aggressive chemicals, their resilience shines. Yet, this intricate elegance comes at a cost. Their complexity translates to a price tag that can bite and sensitivity to extreme environmental conditions, limiting their use in certain applications (Wang R. , 2011).

2) Mechanical membrane

Mechanical membranes, forged in the fires of weaving, sintering and electrospinning, march to a different beat. Their straightforward manufacturing processes translate to cost-effectiveness, making them the budget-conscious choice. Their sturdy frames, built for durability, can withstand the rigors of high pressure and mechanical stress, rendering them ideal for heavy-duty applications. Their larger pores, while limiting their selectivity, also minimize the threat of clogging, making

them maintenance-friendly warriors in the fight against impurities (Seymour, 2011). Mechanical membranes are preferred because of cost-efficiency and durability. Their ability to resist harsh chemical environments makes them suitable for scenarios where chemical stability is paramount.

For now, the membrane previously used other methods but because there are problems with that method such as high cost, environmental impact and limited scalability, then additive manufacturing or 3D printing has become one of the basic candidates as 3D printing manufacturing. 3D printing offers more immediate and diverse benefits for mechanical membranes due to their simpler structure and established applications.

2.3 3D Printing

3 Dimensional (3D) printing or additive manufacturing (AM) technologies produce 3D items from computer-aided design (CAD) models by layering material on top of material until a physical object is formed. While 3D printing technologies have been around since the 1980s (Yanar et al. 2020), recent developments in technology, materials and software have made 3D printing more accessible to a broader variety of enterprises, allowing more and more organizations to employ tools that were previously exclusive to a few high-tech industries.

Professional, low cost desktop and benchtop 3D printers now drive innovation and help enterprises in a variety of industries, including engineering, manufacturing, dentistry, healthcare, education, entertainment, jewellery and audiology (Yanar et al. 2020). All 3D printing procedures begin with a CAD model that is transmitted to software to prepare the design. Depending on the technique, the 3D printer may build the part layer by layer by solidifying resin or sintering powder (Hwa et al. 2018).

2.3.1 Type of 3D Printing

The three most established types of 3D printers for plastics parts are stereolithography (SLA), fused deposition modelling (FDM) and selective laser sintering (SLS). These 3D printing technologies bringing powerful and accessible industrial fabrication tools into the creative hands of professionals around the world (Hwa et al. 2018).

I. Stereolithography (SLA)

Stereolithography (SLA) as shown in figure 2.12, the world's first 3D printing technology, was developed in 1980s (Hwa et al. 2018) and is still one of the most popular among experts. In a technique known as photopolymerization, SLA 3D printers use a laser to convert liquid resin into rigid plastic. Figure 2.12 show the stereolithography (SLA) 3D printing.

SLA resin 3D printers have grown in popularity due to its capacity to create high-accuracy, isotropic and waterproof prototypes and parts in a variety of sophisticated materials with fine details and a smooth surface finish. SLA resin formulas match the optical, mechanical and thermal qualities of conventional, technical and industrial thermoplastics (Hwa et al. 2018).

Resin 3D printing is an excellent choice for highly detailed prototypes that require tight tolerances and smooth surfaces, such as moulds, patterns and functional parts. SLA 3D printers are widely utilized in a variety of industries, including engineering and product design, manufacturing, dentistry, jewellery, model building and education. Stereolithography is suited for rapid prototyping, functional prototyping, concept modelling, short-run production, dentistry applications, jewellery prototypes and casting.

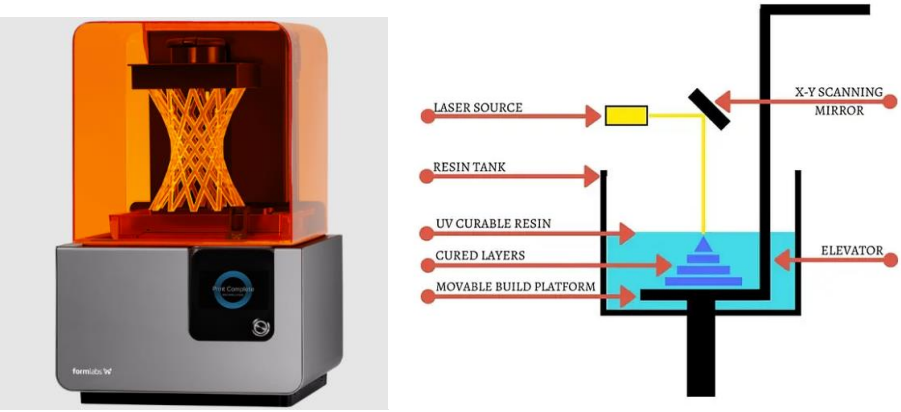

Figure 2.12: Stereolithography (SLA) and the process (manufactur 3d, 2018).

II. Fused Deposition Modelling (FDM)

Fused deposition modelling (FDM) as shown in figure 2.13, commonly known as fused filament fabrication (FFF), is the most popular method of 3D printing among consumers. FDM 3D printers function by extruding thermoplastic filaments such as ABS (Acrylonitrile Butadiene Styrene) and PLA (Polylactic Acid) through a heated nozzle, melting the material and putting the plastic layer by layer to a build platform. Each layer is placed down one at a time until the part is finished.

FDM 3D printers are well-suited for basic proof of concept models, as well as quick and low-cost prototyping of simple parts, such as parts that would generally be machined (Hwa et al. 2018). However, when compared to SLA or SLS, FDM has the lowest resolution and precision, making it unsuitable for printing complicated patterns or objects with intricate elements (Low et al. 2017). Chemical and mechanical polishing procedures can be used to achieve higher-quality finishes. Industrial FDM 3D printers use soluble supports to reduce some of these difficulties and offer a wider selection of engineering thermoplastics (Hwa et al. 2018), but they are also expensive. Fused deposition modelling is appropriate for basic proof-of-concept models and simple prototyping.

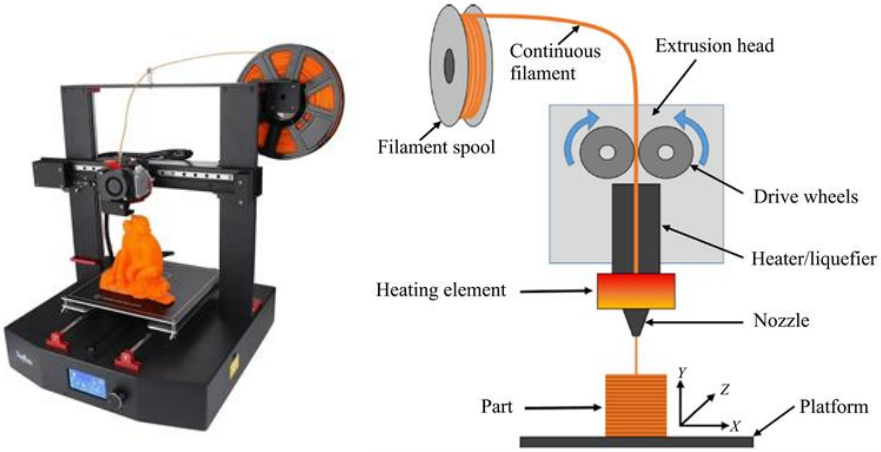

Figure 2.13: Fused deposition modelling (FDM) and the process (Ricoh, 2021).

III. Selective Laser Sintering (SLS)

Selective laser sintering (SLS) 3D printers employ a high-powered laser to sinter tiny particles of polymer powder into a solid structure (Hwa et al. 2018). The unfused powder supports the item during printing, eliminating the need for dedicated support structures. As a result, SLS is perfect for complex geometries such as internal features, undercuts, thin walls and negative features. Parts made with SLS printing have outstanding mechanical properties, with strength comparable to injection-moulded parts(Alahnoori, 2023). Figure 2.14 shows selective laser sintering (SLS) 3D printers.

The most used material for selective laser sintering is nylon, a popular technical thermoplastic with outstanding mechanical qualities. Nylon is lightweight, strong and flexible, as well as resistant to impact, chemicals, heat, UV light, water and dirt (Low et al. 2017). Polyamide-12 that is used to fabricated membrane also commonly known as nylon-12. The combination of low cost per part, high productivity and well-established materials makes SLS a popular choice among engineers for functional prototyping and a cost-effective alternative to injection moulding for limited-run or

bridge manufacturing (Alahnoori, 2023). Selective laser sintering is suited for functional prototyping, end-use products and short-run, bridge, or custom manufacturing. Figures 2.15 and 2.16 show the SLS 3D printing process and its flow.

One advantage of 3D printing technology is the ability to control the pore size and shape of the membranes. The resolution range of 3D printing methods, such as SLS, allows for the creation of membranes with small sized pores at nanometer level, making them suitable for applications involving oil-water separation. It is important to note that although 3D printing offers promising opportunities for membrane fabrication, there are still challenges to overcome. Achieving uniform porosity throughout the membrane structure, ensuring proper interconnectivity of the pores and selecting suitable materials for the desired separation performance are among the key areas of research in this field. SLS 3D printing has emerged as a favoured approach for membrane synthesis, with various advantages. SLS's material diversity, ability to handle complicated geometries, scalability, design freedom, waste minimization and rapid prototyping capabilities make it an appealing alternative for membrane manufacture.

As a conclusion, SLS 3D printing has potential to revolutionize membrane fabrication. The ability to create customized membrane structures with controlled pore sizes and shapes makes it a promising approach for oil-water separation applications. As SLS technology advances, it holds enormous promise to produce high-performance membranes with favourable wettability for behaviour of 3D printed membrane for oil remediation.

Figure 2.14: Selective laser sintering (SLS) (AMFG, 2020).

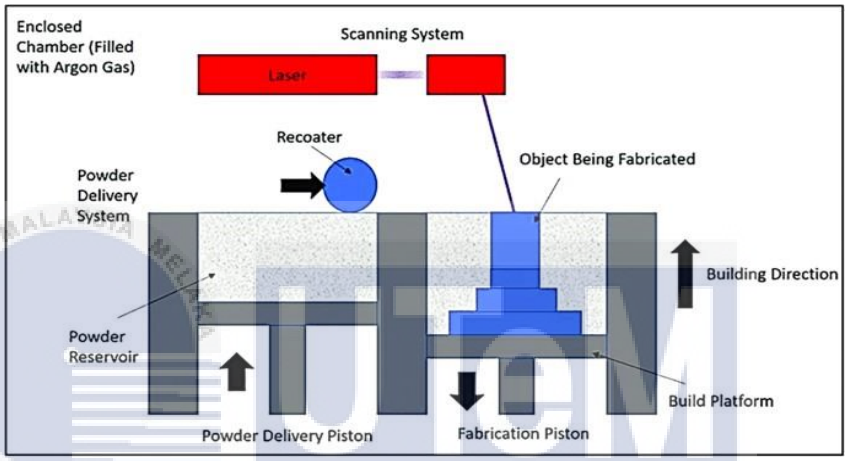

Figure 2.15: Selective laser sintering (SLS) process (M, 2020).

Figure 2.16: SLS 3D printing process flow.

2.4 Wettability

Wettability refers to the ability of a liquid to spread or adhere to a solid surface. It is a property that describes the interaction between a liquid and a solid. The concept of wettability is based on the balance between adhesive forces, which attract the liquid molecules to the solid surface and cohesive forces which attract the liquid molecules to each other (Rbihi et al. 2020). It can be calculated using the contact angle between the liquid and the surface. Surface energy and contact angle are closely connected, meaning that as surface energy increases, the contact angle decreases. The wettability of a solid surface depends on the interplay of forces between the solid, liquid and vapor phases. As shown in figure 2.17, arrows represent these forces. Solid-liquid interfacial tension is the force between solid and liquid molecules. Liquid-vapor interfacial tension is the force between liquid molecules and vapor molecules above the liquid. Solid-vapor interfacial tension is the force between solid molecules and vapor molecules above the solid (Sarkar et al. 2023). There are four types of wettability hydrophilic, hydrophobic, oleophilic and oleophobic.

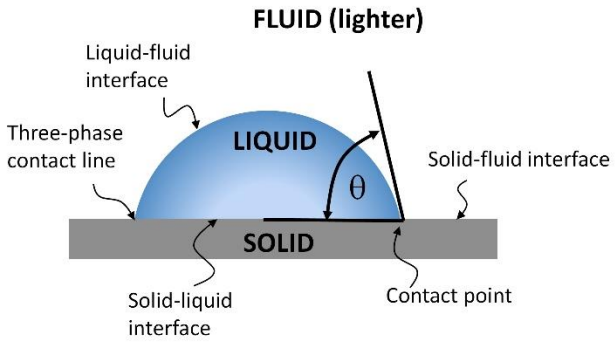

Figure 2.17: Contact angle (Source: www.surfi.mtu.edu)

I. Hydrophilic

Hydrophilic surfaces are those that have a high affinity for water or other polar liquids. Water contact angles on hydrophilic surfaces are less than 90°. When a hydrophilic surface is in contact with water, for example, the water molecules are strongly attracted to the surface and can spread out, resulting in a thin film (Rbihi et al. 2020). This behaviour is due to the presence of polar functional groups or chemical moieties on the surface that can form hydrogen bonds with water molecules.

II. Hydrophobic

Hydrophobic surfaces, on the other hand, reject water or polar liquids. Hydrophobic surfaces have a water contact angle of more than 90°. When water comes into touch with a hydrophobic surface, the droplets tend to bead up and avoid contact with the surface (Sakthivel, 2021). The hydrophobic surface repels water due to its low surface energy and weak interactions with water molecules (Jung and Bhushan, 2009). Hydrophobicity is frequently observed on surfaces made of non-polar or low-polarity materials.

III. Oleophilic

Oleophilic surfaces have an affinity for oil rather than water. Oleophilic surfaces have a lower oil contact angle, typically less than 90° (Kim, Srivastava and Khang, 2022).

The surface energy of the substance determines a surface's affinity for water or oil because oleophilic surfaces have lower surface energy than oleophobic surfaces, oil molecules are more drawn to them. Oleophilic surfaces are therefore perfect for uses like oil-water separation and oil spill remediation (George and Verma, 2022).

Surface chemistry, topography and roughness can all be altered to regulate a material's surface energy. For instance, adding hydrophobic groups to a surface can make it more oleophilicity and adding hydrophilic groups can make it more oleophobicity (Cheng, 2019).

Numerous methods, including chemical modification, physical coating and electrostatic deposition, can be used to create oleophilic surfaces. To add oleophilic functional groups to a material's surface, for instance, researchers have employed chemical modification. The surface chemistry can be tailored to obtain specific oil-water separation properties. (Sun et al. 2020)

Another method for creating oleophilic surfaces is physical coating. This process involves coating a substrate's surface with an oleophilic substance. To maximize the material's effectiveness in separating water and oil, the coating's thickness can be adjusted.

By using electrostatic forces, an oleophilic material layer can be deposited onto a substrate using the technique known as electrostatic deposition. The deposition parameters, which include the applied voltage and deposition duration, can be adjusted to regulate the coating's thickness and characteristics (Cheng, 2019).

To summarise, oleophilic surfaces are the reverse of oleophobic surfaces in that they have an affinity for oil rather than water. A material's affinity for water or oil is determined by its surface energy. Oleophilic surfaces can be created using a variety of methods, including electrostatic deposition, physical coating and chemical modification. It is possible to modify the characteristics of oleophilic surfaces to achieve oil-water separation qualities.

IV. Oleophobic

The term "oleophobic materials" refers to substances that are highly resistant to both oil adherence and penetration because they have a low affinity and repel oil and are opposite to oleophilic surfaces These materials can be used in various applications, like making protective coatings and self-cleaning surfaces, as well as preventing corrosion brought on by oils and other organic molecules. (Peng et al., 2019)

In numerous sectors, the utilization of oleophobic materials is essential. To increase safety and visibility, oleophobic coatings are used on car windows in the automotive industry to prevent the accumulation of oils and debris. Furthermore, oleophobic coatings are used on touchscreens in the electronics industry to stop oil and fingerprint accumulation, which enhances user experience.

The affinity of a material for oil is gauged by the oil contact angle. An oil contact angle larger than 90°, usually in the range of 105° to 120°, characterizes oleophobic surfaces. In other words, because of the high contact angle, oil forms a bead and rolls off the oleophobic surface when it meets it, preventing adhesion and penetration.

Several factors, such as surface roughness, chemical composition and surface energy, influence the oil contact angle of a surface. By adjusting the surface texture, which impacts the surface area and surface energy, one can regulate the roughness of the surface. By adding functional groups that repel oils, the surface's chemical composition can be changed.

Oleophobic surfaces can be produced through a variety of techniques, such as etching, coating deposition and chemical modification. An oleophobic layer is applied to a material's surface using the coating deposition technique. By applying a laser or

chemical to a material's surface, the etching method produces a micro- or nanostructure that repels oils. (Yan et al. 2021).

Overall, wettability is a fundamental concept that governs the interaction between liquids and solids, playing a vital role in numerous practical applications and scientific research areas. The summary of the wettability types is listed in Table 2.1.

Table 2.1: Summary of wettability behaviour

No	Wettability		Description	Contact Angle
I	Hydro	Hydrophilic	Strong attraction between liquid and solid. Liquids spread easily.	 θ < 90°
II		Hydrophobic	Weak attraction between liquid and solid. Liquids bead up.	 θ > 90°
III	Oleo	Oleophilic	Strong attraction between oil and solid. Oils spread easily.	 θ < 90°
IV		Oleophobic	Weak attraction between oil and solid. Oils bead up.	 θ > 90°
V	Super	Super-hydrophobic	Extremely weak attraction between the liquid and the solid surface. Liquids form nearly perfect spheres	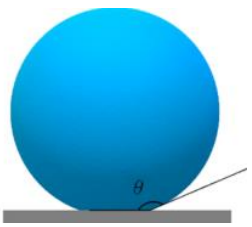 θ > 150°

2.4.1 Factors That Can Affect Wettability

Wettability, or the behaviour of a liquid on a solid surface, is important in a variety of industrial processes and applications. Controlling and modifying wettability is critical for improving the performance of coatings, adhesives, microfluidic devices and biomedical implants (Jung and Bhushan, 2009). Exploring wettability factors and their significance is crucial for comprehending and controlling surface interactions. It can customise surfaces to obtain desired wetting qualities for individual applications by understanding these parameters.

I. Surface Roughness

Surface roughness is an important characteristic that influences wettability greatly. A rough surface improves wetting by increasing the contact area between the liquid and the solid. Micro- or nano-scale roughness patterns create extra energy traps, improving liquid adhesion and spreading (Sakthivel, 2021). Surface roughness alters the effective contact area between the liquid and the solid surface; increasing surface roughness can improve wettability. Surface roughness testing allows researchers to correlate surface roughness parameters with contact angle measurements, providing a deeper understanding of the relationship between surface topography and wetting behaviour.

Surface roughness testing as shown in Figure 2.18, allows for the determination of surface roughness parameters such as average roughness (R_a), root mean square roughness (R_q) and peak-to-valley height (R_z). These factors give quantitative measures of surface imperfections and help to characterise wettability. Researchers can analyse liquid wetting behaviour, such as contact angle and spreading coefficient by measuring surface roughness. This quantitative data aids in the study of wetting

phenomena and aids in the design and development of materials with tailored wetting qualities.

Figure 2.18: Surface roughness tester (techrentals, 2021)

Standard deviation in surface roughness refers to the statistical measure of the variability or dispersion of surface height values within a given surface area. It quantifies the degree of variation or irregularity present in the surface texture. Surface roughness is typically characterized by measuring the vertical deviations of the surface profile from its ideal form. Equation 4.1 describe the equation of standard deviation where σ represent for standard deviation, $\sum$ for summation, x_i individual value, μ mean average and N total number of values.

$$(\sigma) = \sqrt{\frac{[\sum(x_i - \mu)^2]}{N}} \quad (4.1)$$

The standard deviation is calculated by taking the square root of the variance of the surface height values. It provides an indication of the average amount of deviation or variation of individual data points from the mean surface height. In the context of surface roughness, a higher standard deviation indicates a more uneven or rough surface, while a lower standard deviation suggests a smoother and more uniform surface.

By analysing the standard deviation of surface roughness, researchers and engineers can evaluate the consistency and quality of a surface texture. It helps in

assessing the precision of manufacturing processes, comparing different surface finishes and determining the suitability of a surface for specific applications. Additionally, standard deviation can also be used to quantify changes in surface roughness before and after applying various treatments or coatings, providing insights into the effectiveness of surface modifications.

II. Surface Modifications

Surface modifications are an effective way to alter wettability. Coatings, surface treatments and functionalization are examples of procedures that can change the surface characteristics and alter wetting behaviour. For example, putting a hydrophobic coating over a hydrophilic surface can make it hydrophobic, modifying its wetting characteristics(Sakthivel, 2021). These adjustments allow scientists and engineers to produce unique wetting qualities customised to the needs of a certain application.

III. Surface Temperature

Temperature is a parameter that can affect wettability. It has an impact on both the liquid's surface tension and the thermal motion of molecules. Temperature variations can alter the wetting behaviour of liquids on a surface. Temperature increases, for example, might lessen the contact angle and enhance wetness. Understanding the temperature dependency of wettability is critical for designing systems that work under a variety of temperature situations.

IV. Presence of Contaminants

The presence of contaminants on the surface can have a major impact on wettability. Depending on their composition, dust, oils, or surfactants can affect surface chemistry and diminish or increase wetting. For example, the presence of oil can turn a hydrophilic surface hydrophobic, prohibiting wetting. Controlling and reducing the influence of pollutants on the surface is critical for maintaining constant wettability in practical applications.

V. Surface Energy

Surface energy, which is defined as the excess energy at the surface relative to the bulk material, is critical in wettability (Xiao et al. 2022). A high surface energy provides improved wetting by allowing the liquid to spread throughout the surface. The contact between liquid molecules and the solid surface is improved, resulting in better adhesion and wetting behaviour. Surface energy can be adjusted to influence wettability via surface treatments, coatings, or functionalization processes.

2.4.2 Ways to measure contact angle wettability.

Measure of a surface wettability is presented by its contact angle measurement which can be useful information on the interaction of a liquid droplet with a solid surface. To understand wetting behaviour and evaluate surface properties, contact angle measurement must be precise and reliable. There are various method for measuring contact angle and their significance in wettability research such as goniometry, sessile drop, captive bubble, wilhelmy plate and pendant drop. The summary of the wettability types is listed in Table 2.2.

I. Goniometry Method

Goniometry is a traditional and frequently used method for measuring contact angles. It entails taking a picture of a liquid droplet on a solid surface and evaluating the shape of the droplet to estimate the contact angle. Image analysis software is used by goniometers to analyse the droplet image and calculate the contact angle based on geometric principles. Goniometry is a versatile and non-destructive method of measuring contact angles, making it ideal for a wide range of materials and liquids. It is extensively used to characterise surface wettability in research laboratories and industrial settings.

II. Sessile Drop Method

The sessile drop method involves dropping a liquid droplet onto a solid surface and measuring the contact angle formed between the droplet and the surface. This method requires accurate droplet location as well as regulation of environmental conditions such as humidity and temperature (Xiao et al. 2022). Sessile drop contact angle measurements can be performed manually or robotically with a goniometer. This method, which is commonly used in industries such as coatings, textiles and biomedical applications, provides critical insights into the wetting behaviour of a material (Xiao et al. 2022).

III. Captive Bubble Method

The captive bubble method is used to calculate the contact angle of porous or permeable materials. In this method, a gas bubble is trapped within the material's pores and the contact angle at the gas-liquid-solid interface is calculated. The contact angle can be determined using existing models and theories by observing the shape and size

of the bubbles. The captive bubble method allows for the investigation of materials with complex pore topologies and is particularly useful in applications involving membranes, filters and porous coatings.

IV. Wilhelmy Plate Method

The Wilhelmy plate method is commonly used to determine the contact angle of solid materials that are not suitable for droplet-based approaches. The sample is immersed vertically in the liquid in this procedure and a force sensor is used to detect the force exerted on the solid surface as it is withdrawn from the liquid. The contact angle is calculated using the force change as the sample passes through the liquid-air interface. The Wilhelmy plate method is extensively used in the characterisation of powders, fibres and porous materials for measuring contact angles on irregular or rough surfaces.

V. Pendant Drop Method

The pendant drop method is used to determine the contact angle of a liquid droplet suspended from a solid substrate or capillary tube. Examining the droplet shape and the curvature of the liquid-air interface yields the contact angle. When working with high surface tension liquids or minute droplets, this method is quite effective. Pharmaceuticals, microfluidics and surface coating characterisation are all applications of the pendant drop approach.

Table 2.2: List summarize of the method have been described before.

No	Method	Description	Image
I	Goniometry Method	Specialized instruments capture droplet profile directly.	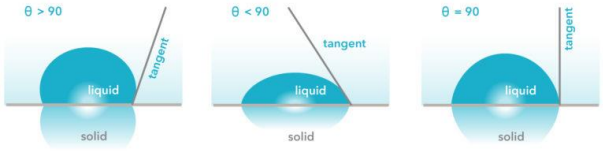
II	Sessile Drop Method	Most common, droplet placed on surface and analyzed.	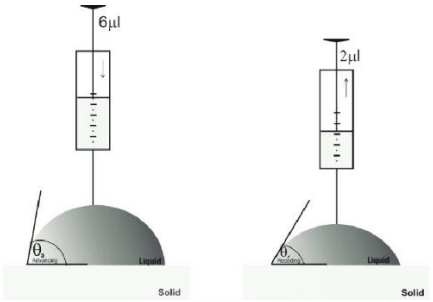
III	Captive Bubble Method	Sample immersed in liquid; air bubble analyzed.	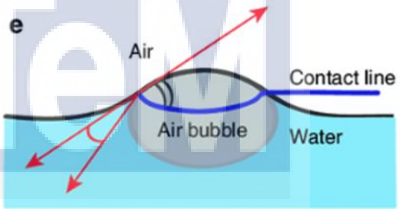
IV	Wilhelmy Plate Method	Solid plate partially immersed, force on plate due to liquid meniscus measured.	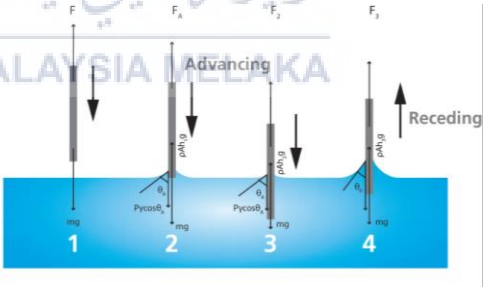
V	Pendant Drop Method	Droplet hangs from needle tip, profile analyzed.	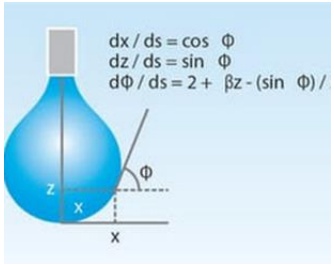

Measuring contact angle can be challenging because it requires a specialized setup that can keep the liquid in place and prevent it from spreading or moving. To measure contact angle, sessile drop method can be considered because it is simple, cost-effective and requires only a small amount of liquid. This method also offers others significant advantages when used for measuring contact angles, which is its non-destructive nature, versatility, accuracy, accessibility and real-time observation capabilities make it a valuable tool for studying wetting behaviour and surface interactions in aquatic environments.

2.5 Summary of Past Research

In this field of wettability of 3D printed membranes, there are various research that had been done. Yuan (2020) had done research on the development of a durable and efficient 3D printed membrane for the separation of oil-water and immiscible organic mixtures. The membrane was constructed by the authors from a powdered polyamide using selective laser sintering (SLS), which guaranteed the material's chemical and mechanical stability. Permeability, mechanical strength and separation efficiency were used to evaluate the membrane's performance. The resulting data showed that the 3D printed membrane had excellent mechanical durability, permeability and separation efficiency. The discussion highlights the potential applications of this novel membrane in various fields such as wastewater treatment and oil spill remediation. According to the study's findings, 3D printed membranes have a great deal of potential for producing adaptable and affordable separation process solutions. In addition, the research findings are corroborated by the work done by Manmadhachary (2021), which highlighted the benefits of 3D printing in producing effective and customized membranes for water treatment uses.

The second research that had been done by Yuan (2017) presented a study on the development of a super-hydrophobic 3D printed polysulfone membrane that exhibits switchable wettability through self-assembled candle soot, aiming to achieve efficient gravity-driven oil-water separation. The research investigated the assumption that the incorporation of self-assembled candle soot on the membrane's surface would result in super-hydrophobic properties, allowing for selective oil-water separation. The results demonstrated that the 3D printed polysulfone membrane with self-assembled candle soot achieves super-hydrophobicity and exhibits efficient gravity-driven oil-water separation with high separation efficiency and flux. The reversible wettability and improved separation performance of this membrane make it a viable candidate for use in wastewater treatment and oil spill cleanup, as discussed in the work. The study concludes that the super-hydrophobic 3D printed polysulfone membrane offers a promising method for efficient oil-water separation processes, opening the door for economical and ecologically friendly solutions in a variety of industries. This is because the membrane's switchable wettability is made possible by self-assembling candle soot.

Another research done by Yuan (2017) focused on the fabrication of polyamide-12 membranes using selective laser sintering (SLS) for microfiltration applications. To produce membranes with exact pore architectures and regulated characteristics, the research investigated the viability of using SLS as a production method. High permeability and retention efficiency are expected to be among the attributes of the polyamide-12 membranes made by SLS that make them ideal for microfiltration. The result showed that, the polyamide-12 membranes made from SLS have the appropriate pore shape and work well for microfiltration. The discussion

highlights the advantages of SLS in creating membranes with tailored properties and the potential applications in various industries requiring efficient microfiltration processes. According to the study's findings, selective laser sintering is a potentially useful method for creating polyamide-12 membranes for microfiltration that offer dependable performance and customization options.

Sakthivel (2021) investigated the use of imidazolium-based ionic liquids (ILs) to change the wettability of carbonate reservoirs. Ionic liquids are salts composed of an organic cation and an inorganic anion, possessing desirable properties for wettability alteration, such as low surface tension, strong rock surface bonding and stability in harsh environments. The experiments conducted by the authors focused on understanding how ILs affect the wettability of carbonate rocks. They discovered that ILs could significantly transform the wettability, making the rocks more water wet. The degree of alteration depended on the specific type and concentration of the IL, as well as the temperature. Additionally, the researchers observed that ILs could enhance oil recovery from carbonate reservoirs. A core flood experiment involved injecting IL into an initially oil-wet carbonate reservoir, leading to a substantial increase in oil recovery. The assumptions underlying this research may include the belief that ILs, due to their specific properties, will effectively alter wettability in carbonate reservoirs. The conclusion drawn from the study is that ILs hold promise as a cost-effective and user-friendly method for wettability alteration in carbonate reservoirs, potentially leading to significant improvements in oil recovery.

Liang et al. (2014) investigates the correlation between the wettability properties and chemical compositions of candle soot. The research aimed to understand how variations in the chemical composition of candle soot affect their wetting behaviour. The assumption was that different chemical components within candle soot contribute to varying degrees of hydrophobic or hydrophilic properties. The study analyzed the wetting characteristics of candle soot through contact angle measurements and investigated the chemical composition using techniques like X-ray photoelectron spectroscopy (XPS) and Fourier-transform infrared spectroscopy (FTIR). The results demonstrated a clear relationship between the chemical composition and wetting behaviour of candle soot. The discussion highlighted the influence of specific chemical groups, such as aromatic and aliphatic hydrocarbons, on the observed wetting properties. The research concluded that the chemical composition of candle soot plays a crucial role in determining their wetting characteristics, offering valuable insights for potential applications in areas such as non-wetting coatings, oil-water separation and surface engineering.

Al Shimmery (2018) focused on the development of 3D printed membranes with improved resistance to fouling. The research aimed to address the issue of fouling, which is a common problem in membrane-based separation processes. Through the utilization of AM techniques, composite membranes were fabricated with the integration of anti-fouling agents. The assumption was that the incorporation of these agents would enhance the membrane's fouling resistance. The results demonstrated that the 3D printed composite membranes indeed exhibit enhanced anti-fouling behaviour compared to conventional membranes. The discussion highlighted the mechanisms behind the anti-fouling properties and potential applications in various

fields such as water treatment and wastewater purification. The research concluded that 3D printed composite membranes with enhanced anti-fouling characteristics offer great potential for improving the efficiency and longevity of membrane separation processes, addressing the challenge of fouling.

Wang (2021) investigated the design and properties of a stainless-steel mesh that exhibits reversible transitions between superoleophobicity (repelling oil) and superhydrophobicity (repelling water). The primary goal was to enhance the efficiency of oil-water separation processes. Results suggested that the designed stainless steel-mesh successfully demonstrated reversible wettability transitions. This implies that the mesh can effectively repel both oil and water, providing a versatile solution for efficient oil-water separation. Assumptions underlying this research might include expectations regarding the stability and durability of the reversible wettability transitions under various conditions. The study also assumed that the designed stainless-steel mesh would offer practical advantages in real-world oil-water separation applications. Conclusions from the references highlighted the potential of the reversible wettability stainless-steel mesh for efficient and versatile oil-water separation. The findings may contribute to advancements in material design for environmental applications, emphasizing the significance of reversible wettability in enhancing separation processes.

CHAPTER 3

METHODOLOGY

3.1 Introduction

This chapter discussed the methodology employed in this research to achieve project's objectives. The methodology for this research involved several activities: a) material preparation, b) material fabrication and coating, c) material characterization and d) procedures of the experiment. The general flow chart is illustrated in Figure 3.1.

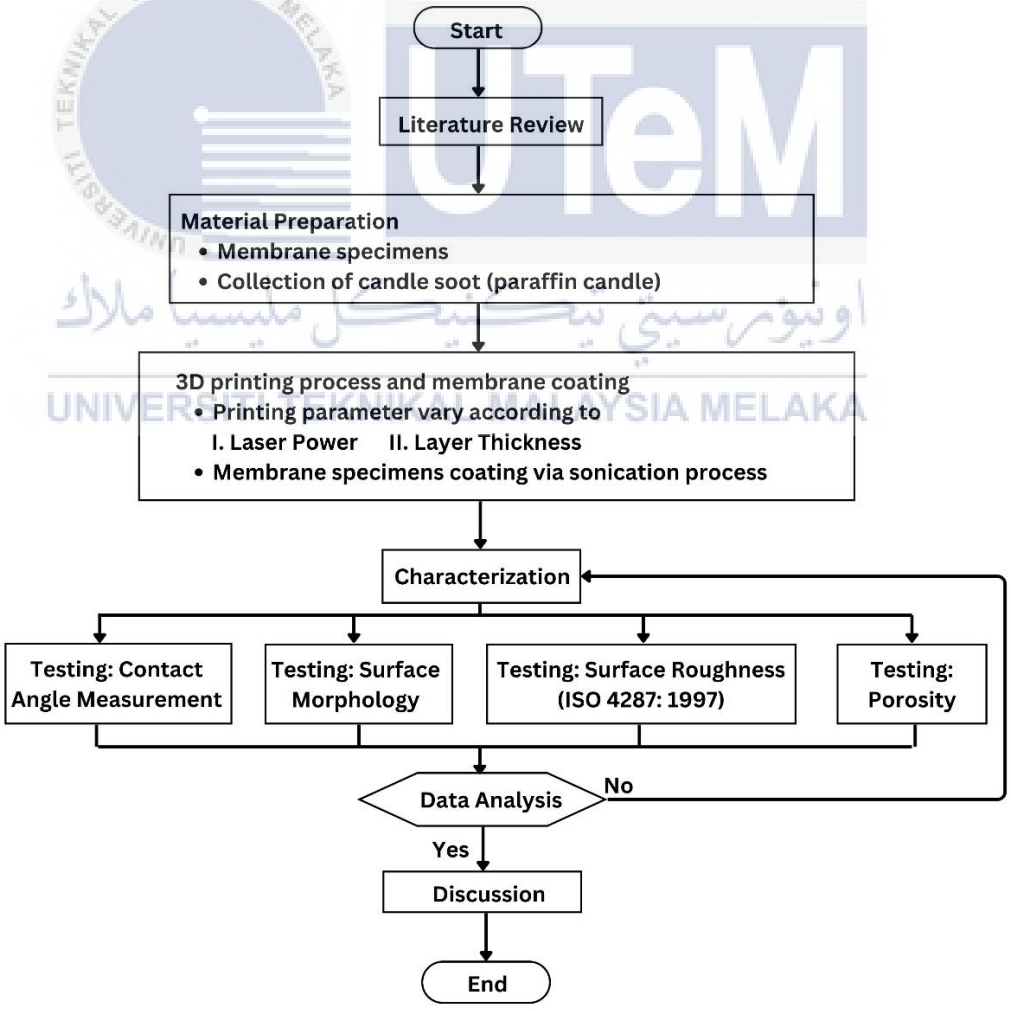

Figure 3.1: General methodology flow chart for this research

3.2 Material Preparation

Material preparation for this research involved the preparation of specimens with specific dimensions. This included the fabrication or shaping of specimens according to the desired specifications, ensuring uniformity and consistency in the experimental setup. Accurate dimensions and well-defined specimen geometry were vital for reproducibility and reliable data analysis. The material preparation also covered the collection process of candle soot, which served as a crucial component for enhancing the properties of the membranes. The process of collecting and preparing the candle soot were discussed, highlighting its importance in achieving the desired membrane characteristics.

3.2.1 Specimen Design and Modelling

A specimen is a sample or physical object used for testing or analysis. In the context of separation procedures, a specimen could be a physical object or component utilized to enhance the separation of water from oil. A specimen could take the form of a 3D printed membrane or filter housing used in a membrane filtration process or a 3D printed skimmer employed to gather oil from the water's surface. The design, material and qualities of the specimen had a considerable impact on the performance and efficiency of the separation process and these parameters were carefully considered and optimized to achieve optimal separation performance.

The specimen were printed by 3D printer before it can be printed, it must be draw in SolidWorks or AutoCAD software, where the specifications such as the desired thickness, pore size and overall dimensions were carefully deliberated to meet the requirements for 3D printing machine. The design, tailored for compatibility with

3D printing machine, was then exported in the suitable file format (e.g., STL). Different design may require for specific testing method to accurately assess the desired properties. The geometries of the specimen shown in Table 3.1.

Table 3.1: Membrane specimens geometries following the testing specifications.

No	Drawing	Geometries	Testing
1	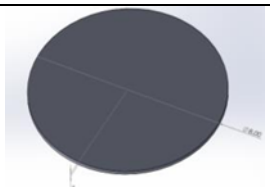	Geometry: Circular Diameter: 8 cm Thickness: 1 mm	1) Surface morphology 2) Surface roughness
2		Geometry: Circular Diameter: 5 cm Thickness: 1 mm	1) Porosity
3	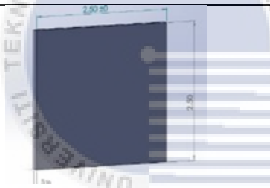	Geometry: Square Diameter: 2.5 cm x 2.5 cm Thickness: 1 mm	1) Dry contact angle measurement

3.2.2 Candle soot collection

The study of wettability frequently included the evaluation of specific materials or compounds such as candle soot. Candle soot is a result of incomplete combustion that occurred when paraffin wax burns inefficiently. It is made up of small carbon particles that could be released into the air and settle on surfaces, resulting in ugly black stains. Aside from its visual impact, soot could impair the wettability features of the candle's surface, potentially impeding the dispersion and absorption of liquids. Collecting candle soot for wettability analysis necessitates meticulous material preparation to achieve accurate and representative results.

Coating candle soot not only improved wettability but also enhanced the visual appeal of paraffin candles. By reducing soot emissions, the candle produces a cleaner flame, creating a more visually pleasing atmosphere. This is particularly important in situations where the candle's appearance and aesthetics played a significant role.

In this project, candle soot particles were obtained by placing a clean metal plate on top of a mid-flame candle for 10 minutes at 2 cm. The candle soot that had been deposited on the metal plate was then scraped off and stored in preparation for polyamide-12 powder modification. Figure 3.2 shows the setup and the collected candle soot.

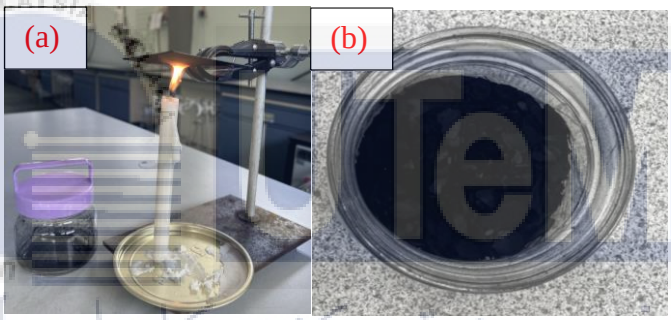

Figure 3.2: Candle soot collection (a) The setup (b) The collected candle soot

3.3 Material fabrication and coating

This section explains the membrane fabrication methods and the process; it also covered coating membrane with candle soot after collection. The application of a thin layer of coating material onto the membrane surface can significantly influence its surface properties, such as hydrophilicity, hydrophobicity, surface charge and chemical interactions.

3.3.1 Printing Process

The specimens drawn in SolidWorks as shown in part 3.2.1 were fabricated in the printing process using SLS 3D printing. Polyamide-12 (PA-12) powder was selected as the powdered material, aligning with the chosen 3D printing method. In the subsequent steps of membrane fabrication, the powder bed was warmed to 169.5 °C prior to the laser exposure. It was then scanned by the laser to create the appropriate geometries as shown in part 3.2.1. The laser power and layer thickness parameters listed in Table 3.2 were used to print the membrane specimens. Figure 3.3 shows SLS printing process.

Table 3.2: SLS printing parameters

Specimens	Parameters				
	Laser Power (Watt)	Layer Thickness/Slicing (mm)	Laser Beam Velocity (m/s)	Hatch Distance (mm)	Chamber Temperature (°C)
Membrane A	70	0.06	7.6	0.30	169.5
Membrane B		0.12			
Membrane C	80	0.06			
Membrane D		0.12			

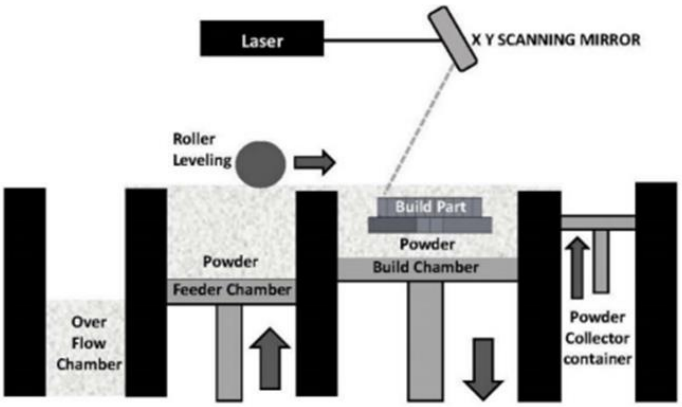

Figure 3.3: SLS printing process

3.3.2 Coating of Polyamide-12 powder with candle soot.

A combination of candle soot/hexane solution (0.1 wt%) was made by combining 80 mg of candle soot particles with 80ml of hexane and sonicating the mixture for 30 minutes. This was done after the candle soot had been removed off the metal plate. Sonication processes are used to disperse and coat the powder particles onto the membrane surface. Sonication helps in achieving uniform dispersion and adherence of the powder, resulting in a consistent coating. After that, the 3D-printed PA-12 membranes were then immersed in the candle soot/hexane solution for 40 minutes under sonication. The membranes were then placed in an oven set at 60°C for 10 minutes to remove the hexane from the surface of the PA-12 membranes. After being washed in hexane to remove the loosely attached candle soot, those PA-12 membranes were then dried in a fume hood at room temperature. Figure 3.4 shows the coating membrane process.

Figure 3.4: Sonication process (a) The mixture of candle soot/hexane solution (b) printed specimen immersed in solution (c) Coated versus non-coated.

3.4 Material Characterization

All specimens with varying 3D printing parameters were characterized as follows:

3.4.1 Surface Roughness

Average surface roughness (R_a) was measured on every printed specimen for both coated and non-coated using a surface roughness tester (Mitutoyo SJ-410) and the ISO 4287: 1997 standard. Readings were obtained at three distinct positions on a 5 cm diameter specimen. Measurements were taken on both the top and bottom surfaces of each specimen, applicable to both coated and non-coated membranes. The built-in, colour LCD display of the Mitutoyo SJ-410 surface roughness measuring tool enabled users to see surface roughness waveforms, as shown in Figure 3.5. In addition to calculating results, the display also showed operators assessed profiles, load curves and amplitude distribution curves. This apparatus could measure in any orientation, including vertical and upside-down. For instance, an optional device that accurately took measures in a variety of scenarios was the height gauge adapter.

Figure 3.5: Mitutoyo SJ-410

3.4.2 Contact Angle Measurement

Surface roughness altered the effective contact area between the liquid and the solid surface, influencing the resulting contact angle. The measurement of the surface contact angle was used to determine wettability. Figure 3.6 and 3.7 show contact angle measurement setup and tested specimens. The steps are listed below:

1. A micro syringe was used to softly deposit water/oil droplets of around 5 µL in volume and a radius of a spherical droplet of approximately 1 mm in an air environment on the specimen.
2. A stabilization time of 15 seconds was given before beginning measurements on the contact angle.
3. Five data points were collected at five different positions on the sample surface and were used to calculate average values. A high-speed camera was used to get a picture of the droplet.

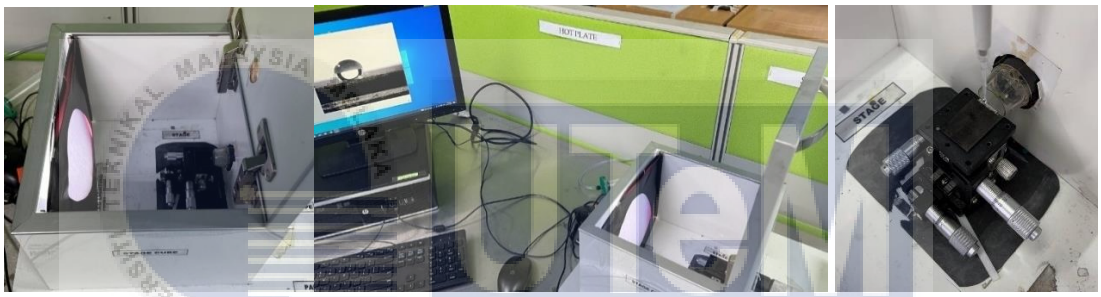

Figure 3.6: Contact angle measurement were conducted using contact angle goniometer.

Type	Specimens ID	Parameters				
		Laser Power (Watt)	Layer Thickness/Slicing (mm)	Laser Beam Velocity (m/s)	Hatch Distance (mm)	Chamber Temperature (°C)
Coated Membrane	CM - 1	70	0.06	7.6	0.30	169.5
	CM - 2		0.12			
	CM - 3	80	0.06			
	CM – 4		0.12			
Non – Coated Membrane	NCM - 1	70	0.06			
	NCM - 2		0.12			
	NCM - 3	80	0.06			
	NCM – 4		0.12			

Figure: 3.7: Tested specimens

3.4.3 Surface Morphology

To acquire a more profound understanding of the structural characteristics and surface morphology of both coated and non-coated membranes for every parameter membrane, scanning electron microscopy (SEM) imaging was utilized. SEM provided the opportunity for high-resolution visualization of the membrane surfaces and cross-sections, offering valuable insights into their microstructure. To enhance sample conductivity and facilitate imaging, a thin platinum coating with a thickness of 5 nm was applied using a sputtering technique. This platinum coating functioned as a conductive layer, allowing for proper electron flow during SEM imaging. Figure 3.8 shows the scanning electron microscopy (SEM) setup.

The SEM imaging was carried out with a Philips Scanning Electron Microscope XL30 FEG. The microscope operated at an acceleration voltage of 5 kV, which proved to be the optimal voltage for imaging the samples under investigation. This voltage setting ensures a balance between image resolution and potential sample damage. Using SEM imaging with the described techniques, thorough examinations of the membrane surfaces, cross-sections and bottom surfaces were performed. This facilitated the observation and analysis of the membrane's microstructure, including aspects such as pore size, surface roughness and overall morphology. The SEM imaging and analysis offered valuable visual insights into the structural properties of the membranes, enabling a more comprehensive evaluation of their suitability and performance for oil-water separation applications.

In this study, the surface morphology of the printed polymer membrane was analyzed using the Scanning Electron Microscope (SEM) JEOL 6010 PLUS, employing magnification settings of 500µm (50x) and 100µm (200x). The image was

visualized with an Electron High Tension (EHT) of 5kV in Secondary Electron Images (SEI) mode.

Figure 3.8: Scanning Electron Microscope (SEM)

3.4.4 Porosity

By checking surface morphology using SEM pictures of the membrane samples, researchers could obtain quantitative data that characterized the material's porosity. It is important to understand the wetting behaviour of materials because the presence and characteristics of pores strongly influence liquid-solid interactions. Quantifying porosity aided in the development of models and predictions related to wettability, enabling the design of materials with desired wetting properties.

Additionally, the porosity of 3D printed specimens for both coated and non-coated membranes was assessed by determining the weight of dry and wet membranes. Initially, the dry specimens were weighed on an analytical balance. Subsequently, the specimens were rinsed with ethanol and washed with deionized water to eliminate residual ethanol, followed by immersion in deionized water for saturation. The weight of the wet specimens was then calculated. The specimen porosity was determined using the formula equation 3.1:

$$P_r = \frac{m_w - m_d}{Ad\rho} \times 100\% \quad (3.1)$$

in which P_r denotes porosity, sample area for membranes is A (cm^2), the thickness of the membrane is d (cm), water has a density of ρ(1 g/cm^3) and the wet and dry membrane masses are m_w and m_d (g), respectively. The porosity data that have been presented are the averages of three samples for each membrane.

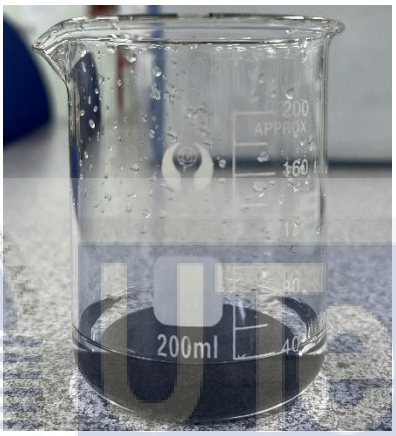

Figure 3.9: Porosity Test

CHAPTER 4

RESULTS AND DISCUSSION

4.1 Surface Roughness Test

Surface roughness testing plays a crucial role in assessing the quality and consistency of 3D printed membranes. The results were shown in Table 4.1 meanwhile graph result shown in Figure 4.1 below.

Table 4.1: Result for surface roughness test for non-coated and coated membrane

Membrane	Surfaces		Laser Power (Watt)	Layer Thickness (mm)	Sample ID	Surface Roughness (*Ra*), µm	Standard Deviation
A	1	Top	70	0.06	A1-NC	9.2860	0.4528
					A1-C	9.9433	0.3108
	2	Bottom			A2-NC	10.3430	0.1655
					A2-C	10.6413	0.4347
B	1	Top	70	0.12	B1-NC	11.2950	0.2512
					B1-C	13.6043	0.6370
	2	Bottom			B2-NC	13.5370	0.2993
					B2-C	14.6337	0.7350
C	1	Top	80	0.06	C1-NC	8.8297	0.2620
					C1-C	9.2790	0.3780
	2	Bottom			C2-NC	9.6373	0.4458
					C2-C	10.2617	0.3017
D	1	Top	80	0.12	D1-NC	9.9357	0.2415
					D1-C	10.4053	0.3859
	2	Bottom			D2-NC	10.4603	0.5558
					D2-C	11.4291	0.4822

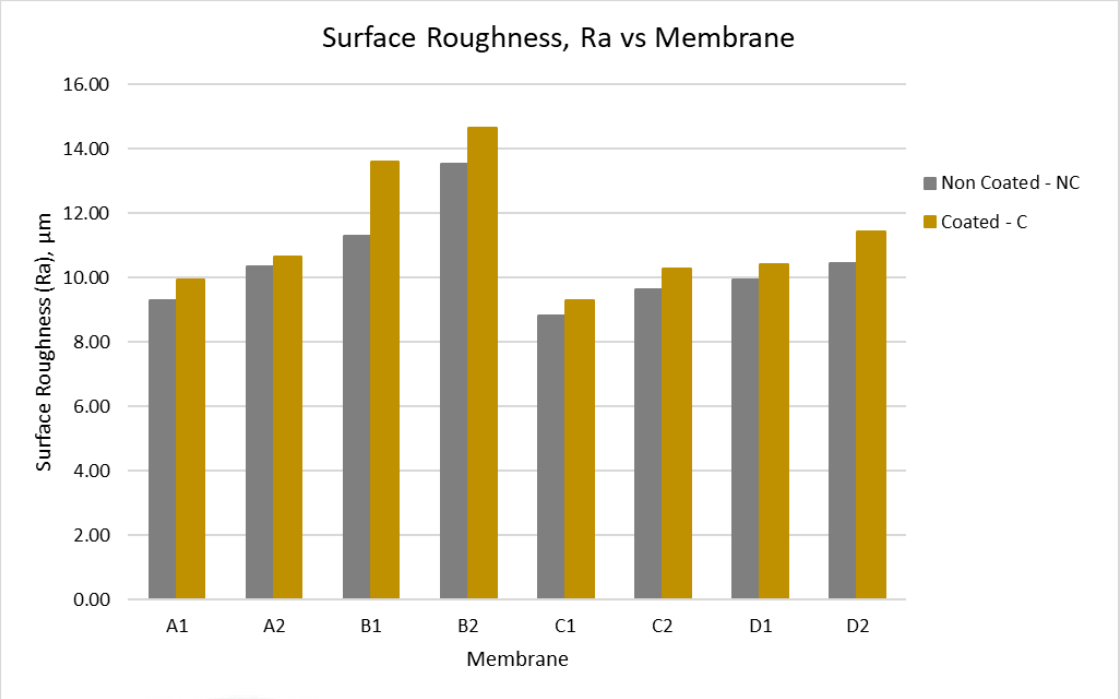

NC – NON-COATED	A – Laser Power 70Watt, Layer Thickness 0.06mm
C – COATED	B – Laser Power 70Watt, Layer Thickness 0.12mm
1 – TOP	C – Laser Power 80Watt, Layer Thickness 0.06mm
2 – BOTTOM	D – Laser Power 80Watt, Layer Thickness 0.12mm

Figure 4.1: Graph showing the results surface roughness for non-coated and coated membrane.

The resulting surface roughness for both non-coated and coated membranes can be attributed to a confluence of influential factors pertaining to laser processing parameters and material characteristics. Based on Figure 4.1 above, between 16 specimens, coated specimen with parameters of 70W laser power and 0.12mm layer thickness was observed to have higher roughness than other samples. This is because the lower laser power might not provide sufficient energy to thoroughly melt and fuse the material, particularly with the thicker layer requiring more energy for effective processing, so it leads to uneven surfaces and increased roughness. Meanwhile, non-coated specimen with parameters of 80W power with a 0.06mm layer appears to have lower roughness than other samples due to the increased power compensates for the

reduced layer thickness and fostering improved material fusion, resulting in a smoother surface (Barrios and Romero, 2019; Petzold et al. 2019).

Furthermore, the influence of layer thickness on roughness is evident. Thinner layers (0.06mm) result in smoother surfaces because each layer contain less material. A thicker layer (0.12mm) may contribute to increased roughness due to the larger amount of material being processed (Khanna, 2021). Rough surface can help to improve the filtration performance of a membrane by trapping more particles.

The candle soot coating introduces additional variables. Coated membrane has higher roughness compared to non-coated membrane because candle soot is made up of carbon nanoparticles (Hussein, Wais and Khedir, 2022). These nanoparticles form a loose network structure on the surface of the membrane, which increase the surface roughness. The thicker layer of candle soot for (0.12mm) layer may lead to an uneven surface, contributing to higher roughness because of coating material (Shooto and Dikio, 2011).

Another observation worths nothing is that the bottom surface membrane results higher roughness compared to top surface membrane due to minimal energy received during printing process. The minimal energy received by the bottom surface of the membrane results in a rough surface compared to the top surface of the membrane. The polymer type, particle size, morphology and density of the powder bed may influence the value of the minimal energy (Yuan et al. 2020).

4.2 Contact Angle Test

In determining the wettability of the membrane, water contact angle measurement was evaluated for top and bottom surfaces of both coated and non-coated membranes. In the oil remediation, the hydrophobicity of a membrane is a crucial factor. As presented in Table 4.2, the water contact angle for all the specimens was above 90° which has resulted in a hydrophobic behaviour. The result and image of contact angle measurement were depicted in Table 4.3 and Table 4.4.

Table 4.2: Result for contact angle test for non-coated and coated membrane

Membrane	Surfaces		Laser Power (Watt)	Layer Thickness (mm)	Sample ID	Contact Angle (°)	Standard Deviation
A	1	Top	70	0.06	A1-NC	135.9	1.3254
					A1-C	140.4	2.8163
	2	Bottom			A2-NC	138.0	1.3761
					A2-C	146.0	1.0483
B	1	Top	70	0.12	B1-NC	145.3	0.7536
					B1-C	150.8	2.7182
	2	Bottom			B2-NC	149.0	1.3262
					B2-C	151.9	1.5683
C	1	Top	80	0.06	C1-NC	133.9	1.2041
					C1-C	137.3	1.5250
	2	Bottom			C2-NC	137.2	1.4252
					C2-C	141.4	1.6542
D	1	Top	80	0.12	D1-NC	138.2	1.6895
					D1-C	142.7	2.4769
	2	Bottom			D2-NC	139.6	2.0441
					D2-C	145.3	0.7361

1) Non-coated Membrane

Table 4.3: The mean values of water contact angle for non-coated membrane

Laser Power (Watt)	Layer Thickness (mm)	Top	Bottom
70	0.06	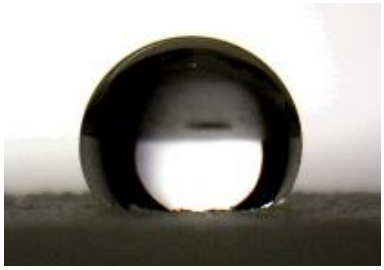	
		θ = 135.9°	θ = 138.0°
	0.12	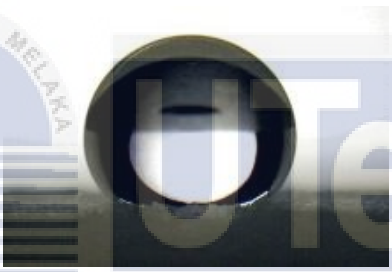	
		θ = 145.3°	θ = 149.0°
80	0.06		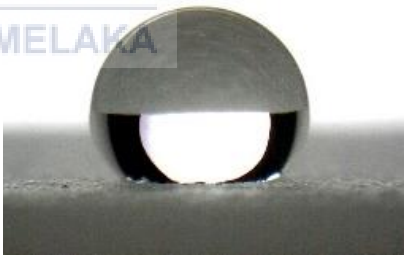
		θ = 133.9°	θ = 137.2°
	0.12	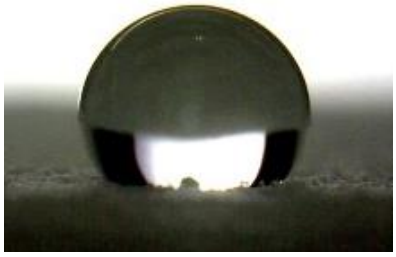	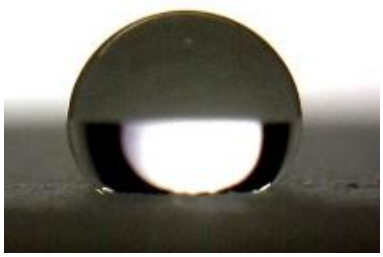
		θ = 138.2°	θ = 139.6°

2) Coated Membrane

Table 4.4: The mean values of water contact angle for coated membrane

Laser Power (Watt)	Layer Thickness (mm)	Top	Bottom
70	0.06		
		θ = 140.4°	θ = 146.0°
	0.12	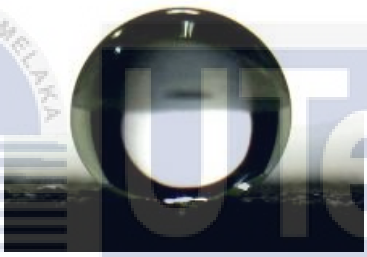	
		θ = 150.8°	θ = 151.9°
80	0.06		
		θ = 137.3°	θ = 141.4°
	0.12	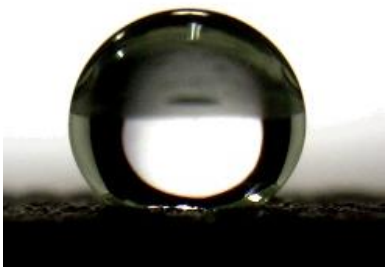	
		θ = 142.7°	θ = 145.3°

Table 4.2 shows that the specimen with laser power 70W and layer thickness 0.12mm has higher water contact angle among other samples. This is because the thicker layer (0.12mm) created at 70W may result in a rougher surface compared to the thinner layers (0.06mm). Increased surface roughness can contribute to a higher contact angle as it provides more opportunities for the liquid (e.g., oil) to bead up rather than spread out (Yuan *et al.*, 2020).

Table 4.2 above shown the coated membrane's water contact angle was higher than the non-coated membrane's. This is because specific chemical composition of the coating can significantly impact the contact angle. If the coating contains hydrophobic materials likes candle soot, it will tend to repel water, resulting in a higher contact angle (Mulay et al. 2019). Non-coated membranes may be tailored to have a surface chemistry that favours interactions with water molecules, leading to lower contact angles with water (Chen et al. 2022).

Furthermore, from the Table 4.2, it is shown that the top surface of the coated membrane has higher contact angle than the non-coated membrane, the trend is similar for the bottom part which showed coated membrane has higher contact angle. It is proven that the use of the carbon nanoparticle from the candle soot coating on the membrane can enhance the hydrophobicity which make it close to superhydrophobic behaviour. Yuan et al., (2017), mentioned that the roughness of both top and bottom surfaces for the polysulfone membrane was different as the water contact angle for the bottom surface was larger than the top. It can be seen the contact angle also can be affected by the texture and roughness of the surfaces. Jothi Prakash and Prasanth (2021) reported that the surface characteristics such as surface roughness, surface energy and porosity all have an impact on liquid wettability on the surface in terms of the liquid contact angle values.

4.2.1 The effect of surface roughness and contact angle on wettability

A correlation investigation was conducted to establish the relationship between the contact angle and surface roughness of both non-coated and coated surfaces, considering both the top and bottom surfaces. The findings are illustrated in Figure 4.2 and Figure 4.3.

1) Non Coated Membrane

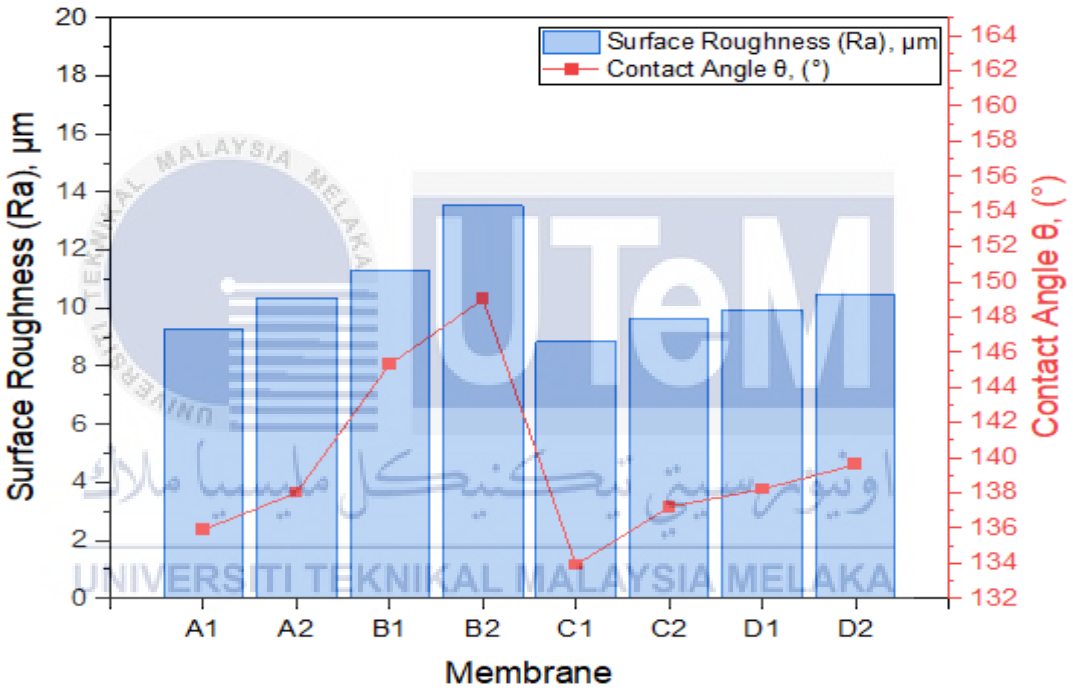

1 – TOP 2 – BOTTOM	A – Laser Power 70Watt, Layer Thickness 0.06mm B – Laser Power 70Watt, Layer Thickness 0.12mm C – Laser Power 80Watt, Layer Thickness 0.06mm D – Laser Power 80Watt, Layer Thickness 0.12mm

Figure 4.2: The correlation between surface roughness and contact angle for non-coated membrane

2) Coated Membrane

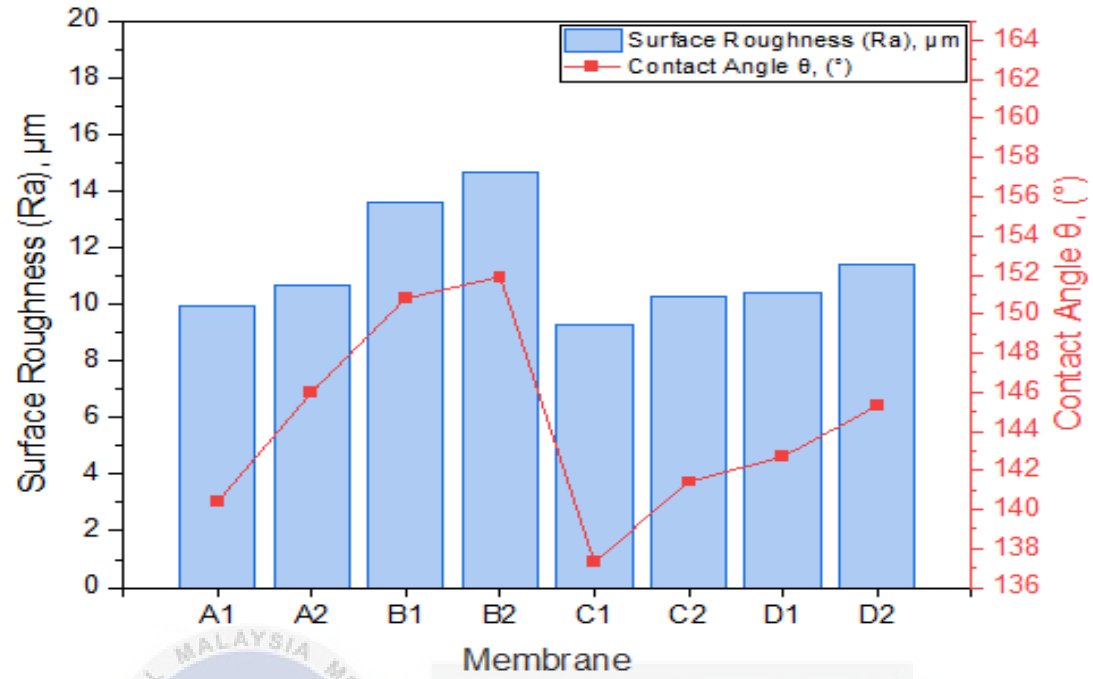

1 – TOP 2 – BOTTOM	A – Laser Power 70Watt, Layer Thickness 0.06mm B – Laser Power 70Watt, Layer Thickness 0.12mm C – Laser Power 80Watt, Layer Thickness 0.06mm D – Laser Power 80Watt, Layer Thickness 0.12mm

Figure 4.3: The correlation between surface roughness and contact angle for coated membrane

According to the results, the contact angle of the membrane was influenced by the surface roughness. The higher the roughness, the higher the contact angle which results in low wettability. The roughness of the surface was significantly affected by the printing process which different energy received by top and bottom surfaces. Besides, the roughness of the membrane was also affected by the modifications that had been made by the deposition of the candle soot coating. Since the candle soot layer comprises hydrocarbons with low surface energy, molecules in water droplets are more attracted to each other than to the surface, resulting in poorer wettability (Rasouli *et al.*, 2021).

Surfaces with low wetting properties will allow oil-water mixture to separate the substances which oil will go through the surface while the water will be repelled. The surface's hydrophobicity increases, resulting in a larger contact angle. As mentioned by Saji (2021), higher surface roughness, nano/micro-hierarchical surface structures, surface reduction procedures (removal of hydrophilic surface groups) and additional low surface energy treatments can enhance hydrophobicity which results in higher contact angle values.

In summary, the contact angle testing results demonstrated varying degrees of hydrophobicity among the different surfaces of the 3D printed membranes. The choice of materials, including the presence of coatings, influenced the wetting behaviour of the surfaces. These findings provide valuable insights for tailoring the membrane properties and optimizing their performance in specific applications that require controlled wetting characteristics.

4.3 Surface Morphology Test

The SEM machine provided magnified surface morphology details in Table 4.5 and Table 4.6, while the test results are presented in Table 4.7 through Table 4.14.

Table 4.5: Top surface membranes magnification

Membrane	Surfaces		Laser Power (Watt)	Layer Thickness (mm)	Sample ID	Magnification
A	1	Top	70	0.06	A1-NC	50
					A1-NC	200
					A1-C	50
					A1-C	200
B	1	Top	70	0.12	B1-NC	50
					B1-NC	200
					B1-C	50
					B1-C	200
C	1	Top	80	0.06	C1-NC	50
					C1-NC	200
					C1-C	50
					C1-C	200
D	1	Top	80	0.12	D1-NC	50
					D1-NC	200
					D1-C	50
					D1-C	200

Table 4.6: Bottom surface membranes magnification

Membrane	Surfaces		Laser Power (Watt)	Layer Thickness (mm)	Sample ID	Magnification
A	2	Bottom	70	0.06	A2-NC	50
					A2-NC	200
					A2-C	50
					A2-C	200
B	2	Bottom	70	0.12	B2-NC	50
					B2-NC	200
					B2-C	50
					B2-C	200
C	2	Bottom	80	0.06	C2-NC	50
					C2-NC	200
					C2-C	50
					C2-C	200
D	2	Bottom	80	0.12	D2-NC	50
					D2-NC	200
					D2-C	50
					D2-C	200

NC – NON-COATED

C – COATED

1) Non-coated Membrane

Table 4.7: The morphology of non-coated membrane surfaces (70W) under SEM

Laser Power (Watt)	Layer Thickness (mm)	Top	Bottom
70	0.06	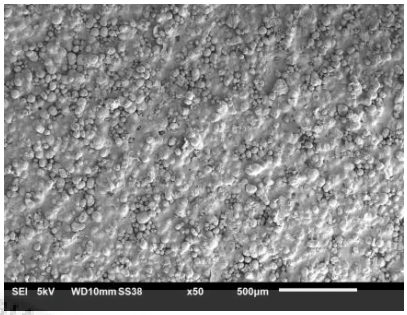	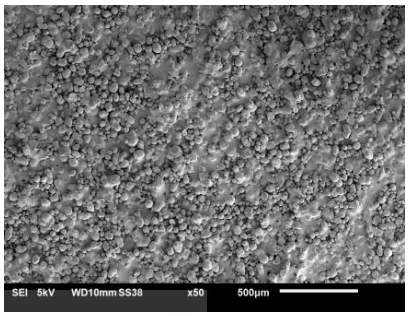
		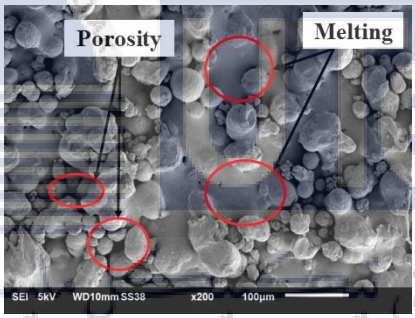	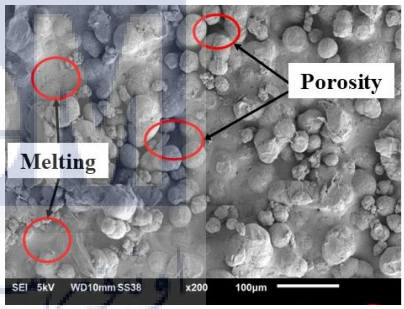
	0.12	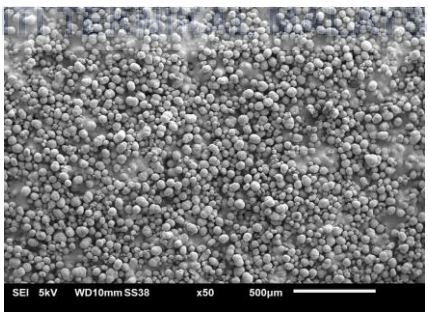	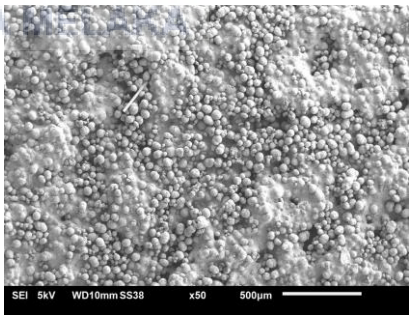
		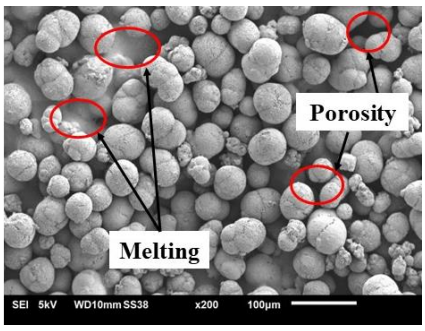	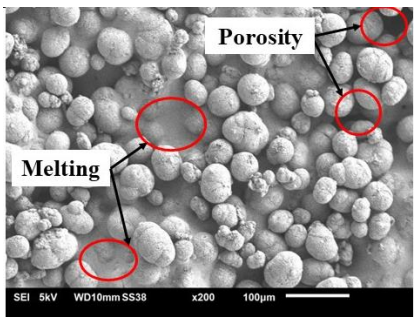

Table 4.8: The morphology of non-coated membrane surfaces (80W) under SEM

Laser Power (Watt)	Layer Thickness (mm)	Top	Bottom
80	0.06	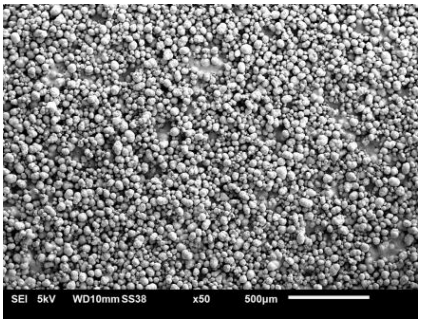	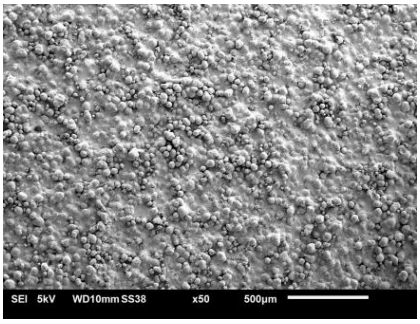
		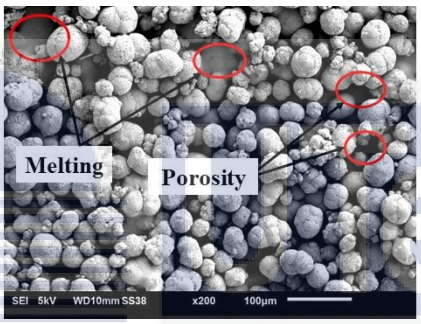	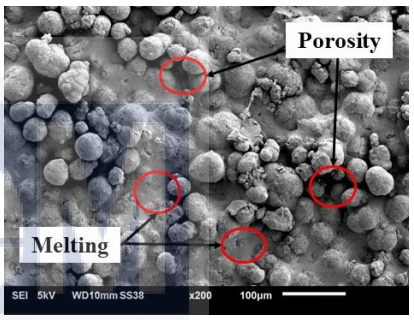
	0.12	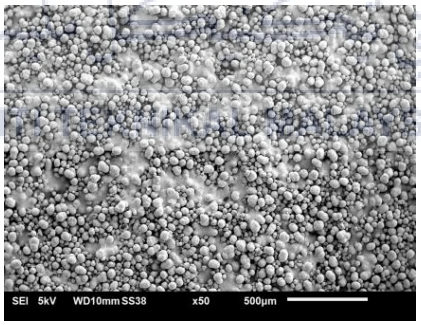	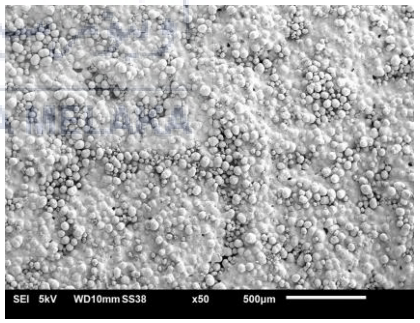
		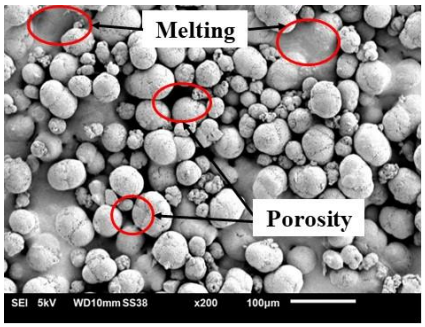	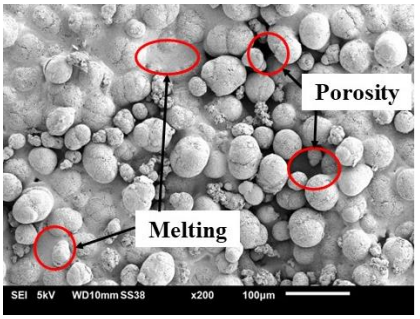

2) Coated Membrane

Table 4.9: The morphology of coated membrane surfaces (70W) under SEM

Laser Power (Watt)	Layer Thickness (mm)	Top	Bottom
70	0.06	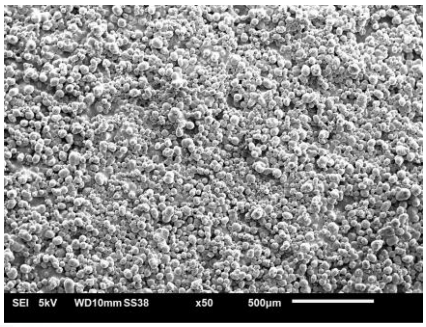	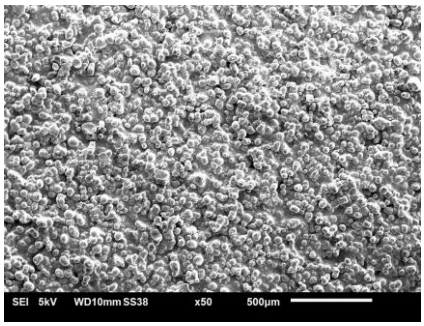
		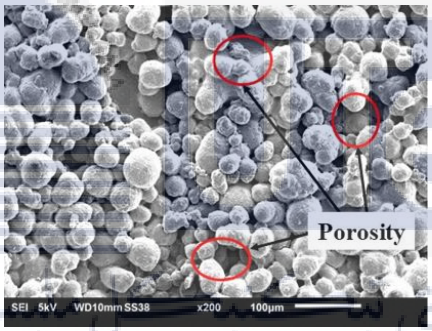	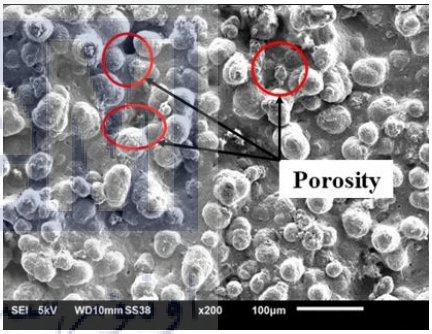
	0.12	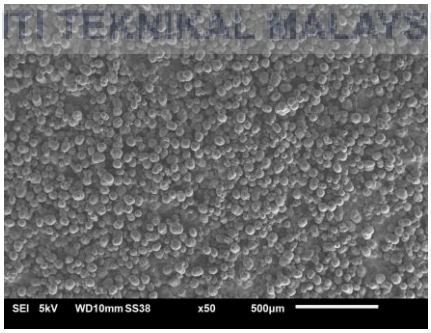	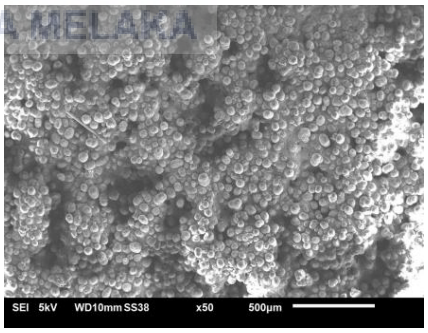
		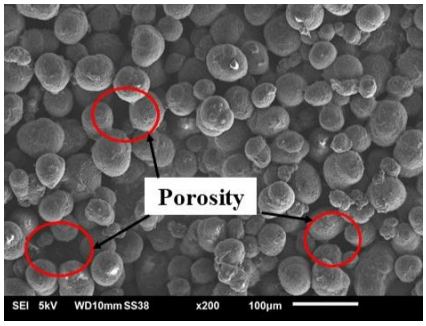	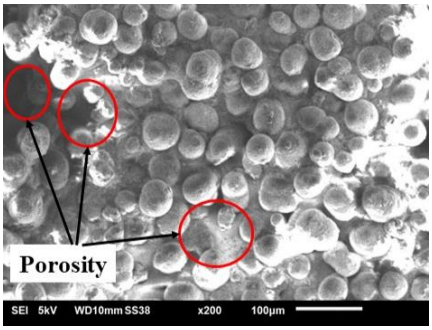

Table 4.10: The morphology of coated membrane surfaces (80W) under SEM

Laser Power (Watt)	Layer Thickness (mm)	Top	Bottom
80	0.06	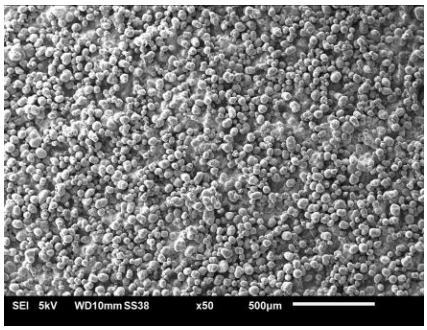	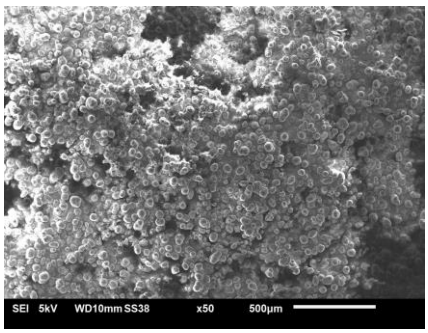
		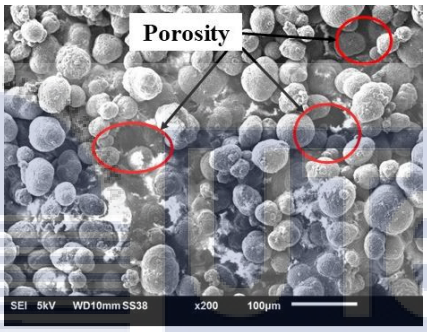	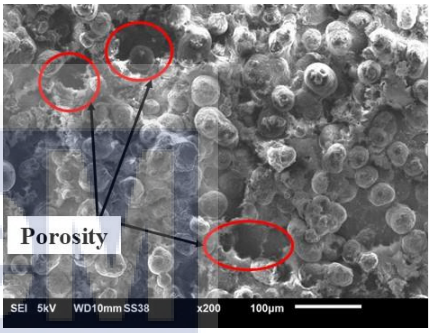
	0.12	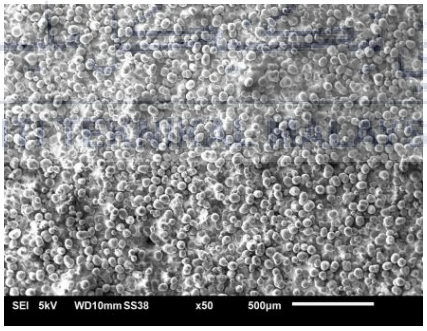	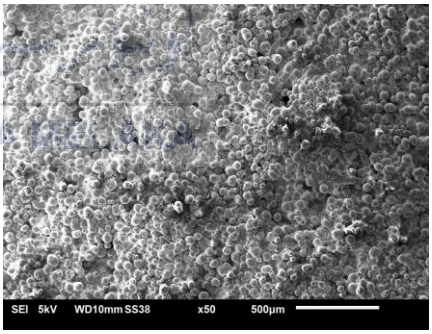
		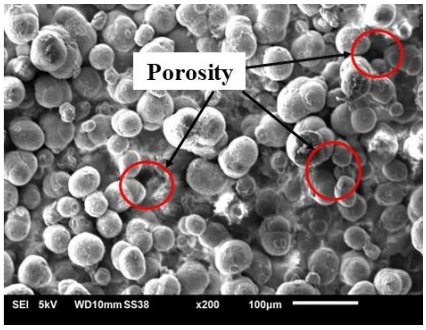	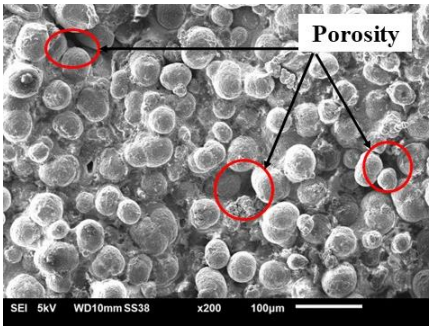

Based on Table 4.7 to 4.10, the SEM results show that bottom surface specimens have bulking melting or even and more pores which causes higher surface morphology compared to the top surface specimen for both coated and non-coated membrane. This is due to the variation of energy absorbed by both surfaces during the sintering process. Sintering requires a particular amount of laser power because of the laser powder interaction, which varies depending on the layer thickness (Golhin *et al.*, 2023). It is noteworthy that the energy distribution from the laser power during the printing process influences the surface quality of the printed parts.

Furthermore, based on the Table 4.7 and Table 4.8, it shown that bottom surface for non-coated uneven melting and clustered due to the coalescence behaviour of the PA-12 powder during the printing process by SLS (Yuan et al. 2017). The surface of the powder bed absorbs the greater energy from the laser during selective laser sintering, generating the top layer of the membrane and is substantially reduced as it goes down to the powder bed. The remaining laser power leads to the partial melting of polymer particles at a specific depth in the powder bed, which results in deficient coalescences of the particles at the bottom layer of the membrane; this is because the full amount of laser energy is incapable to go through into the deeper depth of the bed (Masiagutova, 2021; Yuan et al., 2020). So, it will cause uneven distributions of deposited particles and aggregated structures compared to top surface for non-coated which is even. Average surface roughness is important to observe surface with different position.

SEM analyses in Table 4.7 to 4.10 illustrates the sizes and number of pores on top surface are smaller and fewer to be compared the bottom surface for both non-coated and coated membranes, resulting in a smoother surface.

3) Top Surface Membrane

Table 4.11: The morphology of top membrane surfaces (70W) under SEM

Laser Power (Watt)	Layer Thickness (mm)	Non-coated	Coated
70	0.06	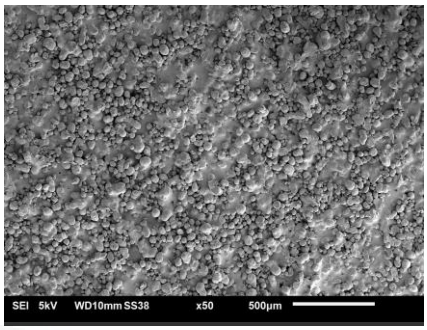	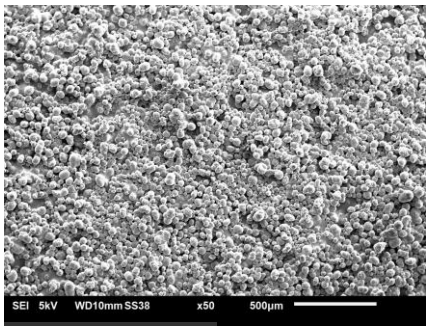
		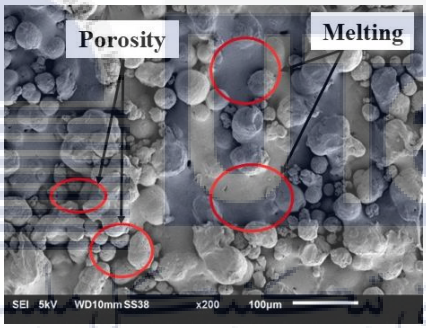	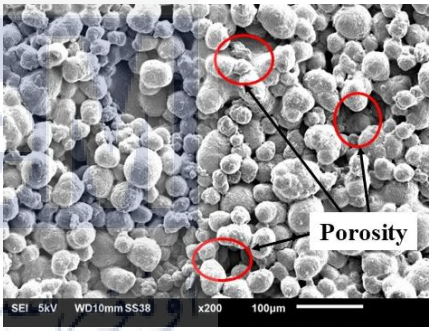
	0.12	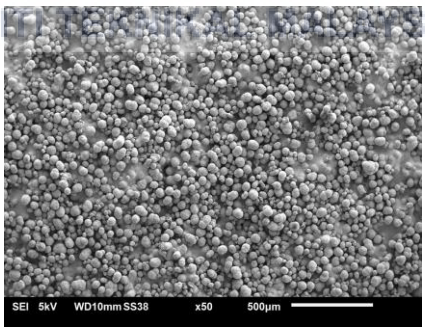	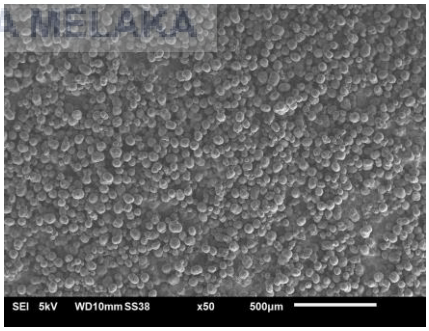
		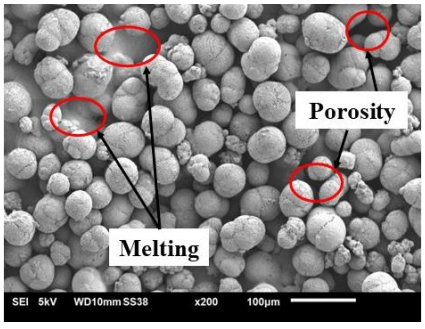	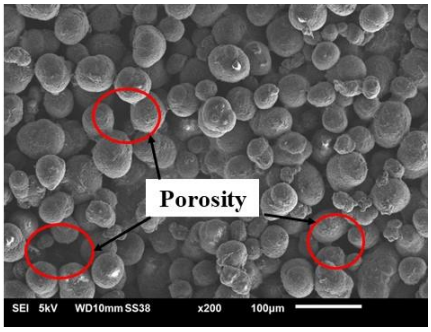

Table 4.12: The morphology of top membrane surfaces (80W) under SEM

Laser Power (Watt)	Layer Thickness (mm)	Non-coated	Coated
80	0.06	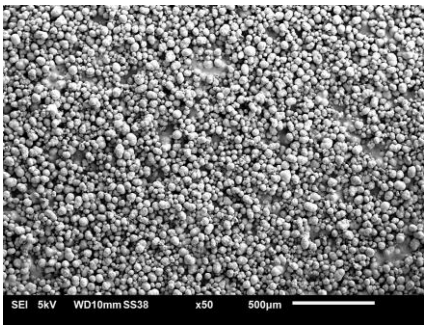	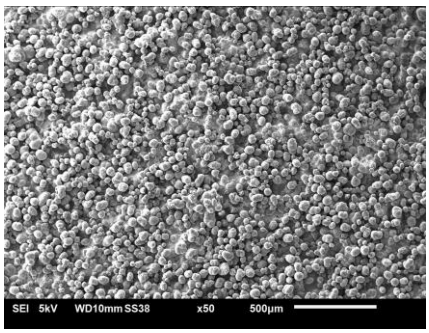
		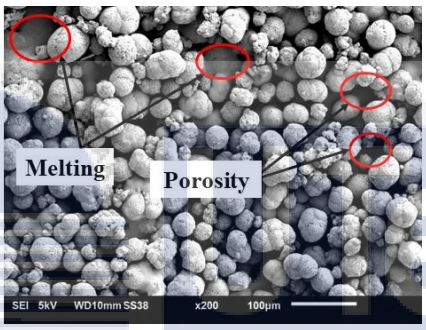	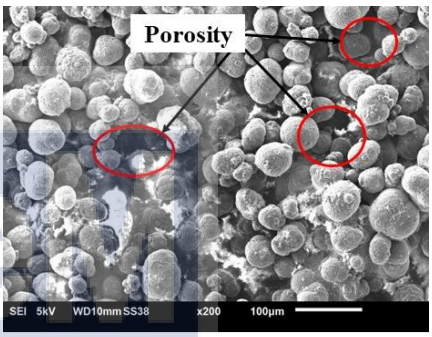
	0.12	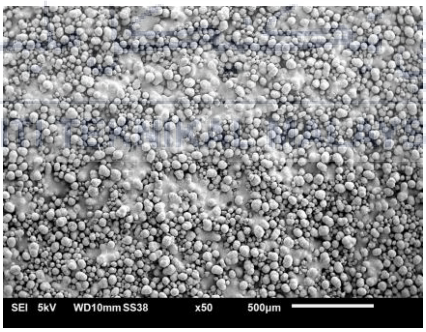	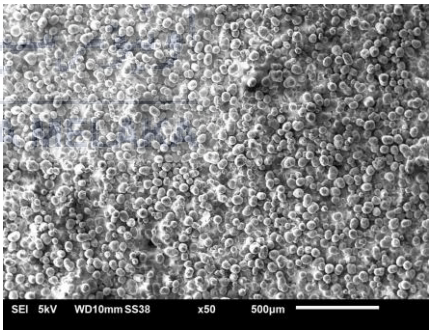
		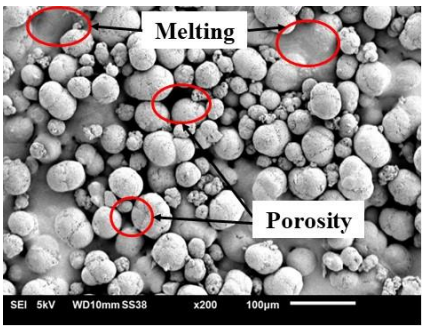	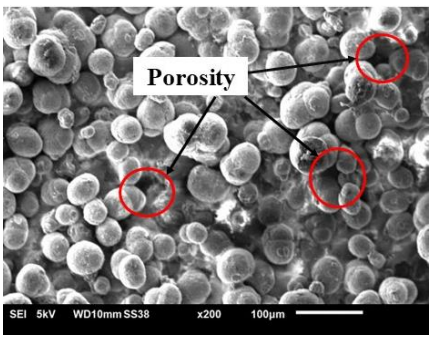

4) Bottom Surface Membrane

Table 4.13: The morphology of bottom membrane surfaces (70W) under SEM

Laser Power (Watt)	Layer Thickness (mm)	Non-coated	Coated
70	0.06	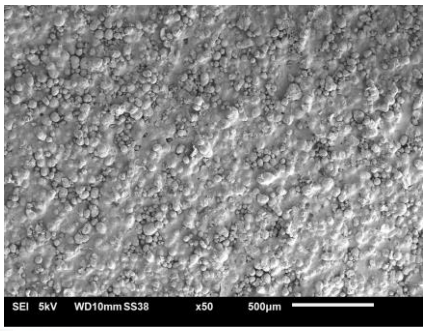	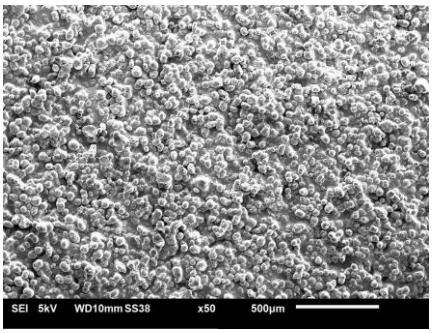
		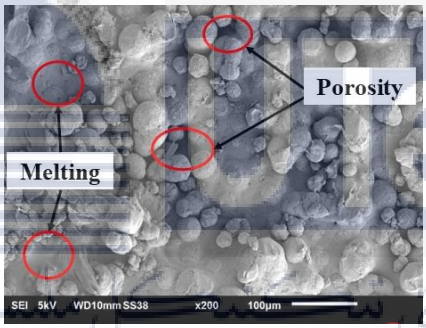	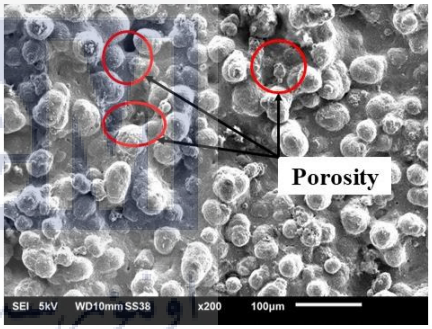
	0.12	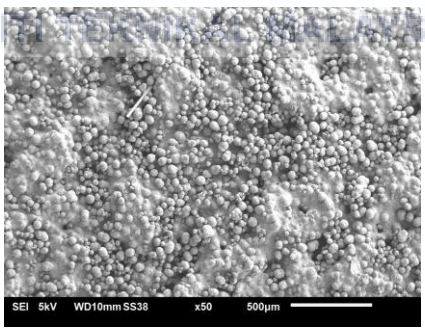	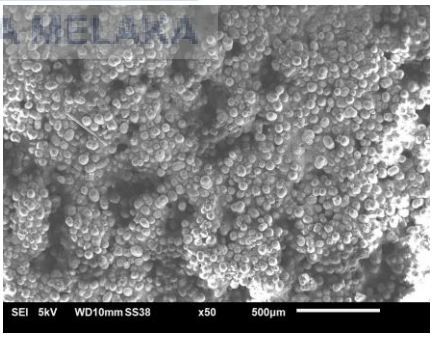
		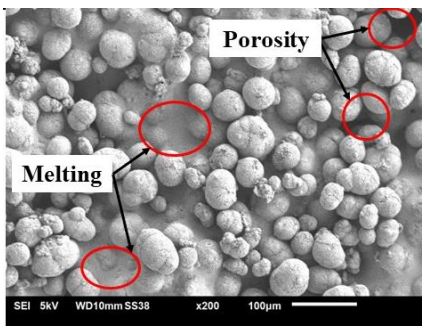	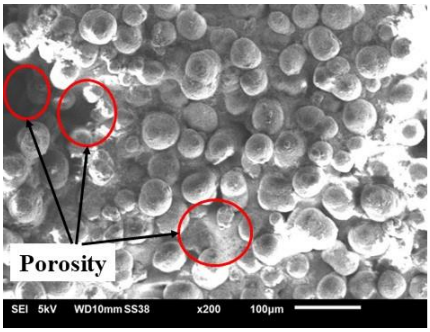

Table 4.14: The morphology of bottom membrane surfaces (80W) under SEM

Laser Power (Watt)	Layer Thickness (mm)	Non-coated	Coated
80	0.06	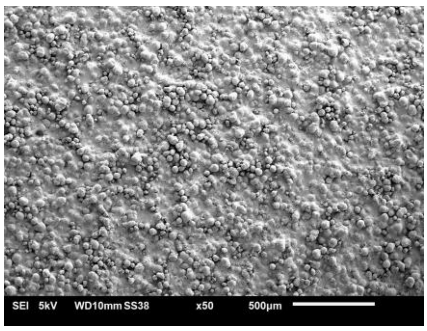	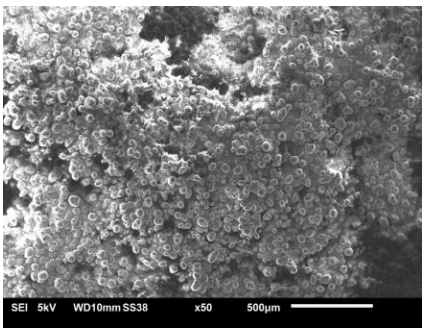
		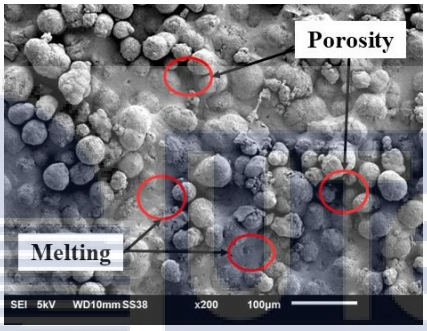	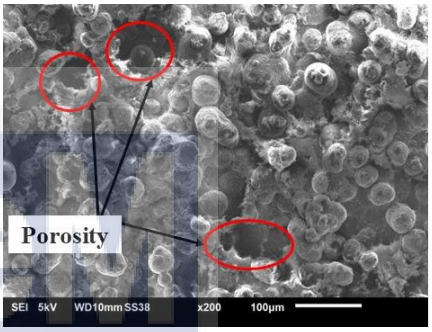
	0.12	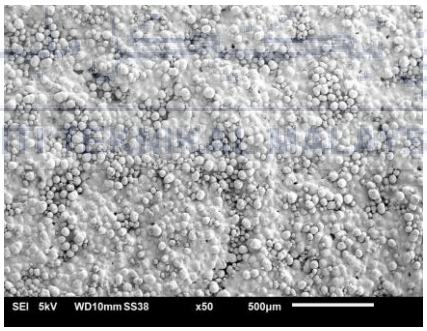	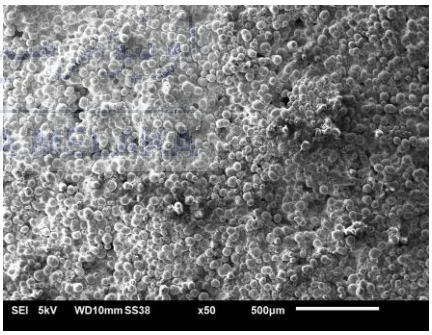
		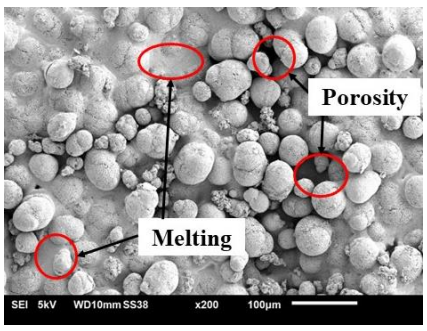	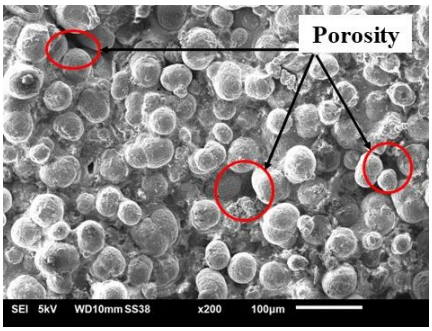

The SEM results based on Table 4.11 to Table 4.14 show that the non-coated membrane exhibited more melting and fewer pores on the surface compared to the coated membrane for both top and bottom. Thus, more melting and fewer pores on the surface resulted in lower average surface roughness (Omar et al. 2022; Yuan et al. 2017).

Meanwhile, the coated specimens shown that that the implementation of candle soot coating amplifies the pore sizes on the membrane surfaces. Yuan et al (2020) discovered that more porous structure generated on the coated membrane due to the candle soot coating layer, which inhibited the coalescence of molten polyamide particles. This structure facilitates the selective passage of water while blocking the passage of oil droplets, enabling efficient oil-water separation.

On the other hand, the rougher and more irregular bottom surface morphology of the coated may provide advantages in terms of increased surface area and potential for higher oil adsorption capacity. The presence of aggregated structures and rough patches can create microscale and nanoscale surface features that enhance the interactions with oil droplets, improving the oil capture and separation efficiency.

4.4 Porosity Test

Porosity is a crucial parameter in membrane performance as it directly affects the membrane's ability to separate fluids. In this study, four different characterizations of 3D printed membranes with their modification for non-coated and coated were tested to obtain the porosity result. The results were shown in Table 4.15 meanwhile graph results shown in figure 4.4.

Table 4.15: Result for porosity test for non-coated and coated membrane

Sample	Laser Power (Watt)	Layer Thickness (mm)	Modification	Sample ID	Average m_d	Average m_w	Porosity (%)
A	70	0.06	Non-coated	A-NC	2.2874	2.3769	13.8273
			Coated	A-C	2.2329	2.50747	13.9853
B	70	0.12	Non-coated	B-NC	1.7258	2.1074	19.4398
			Coated	B-C	1.7257	2.1649	22.3700
C	80	0.06	Non-coated	C-NC	2.5357	2.7690	11.8836
			Coated	C-C	2.5337	2.8164	14.3978
D	80	0.12	Non-coated	D-NC	1.8646	2.1352	13.7782
			Coated	D-C	1.8707	2.1613	14.8069

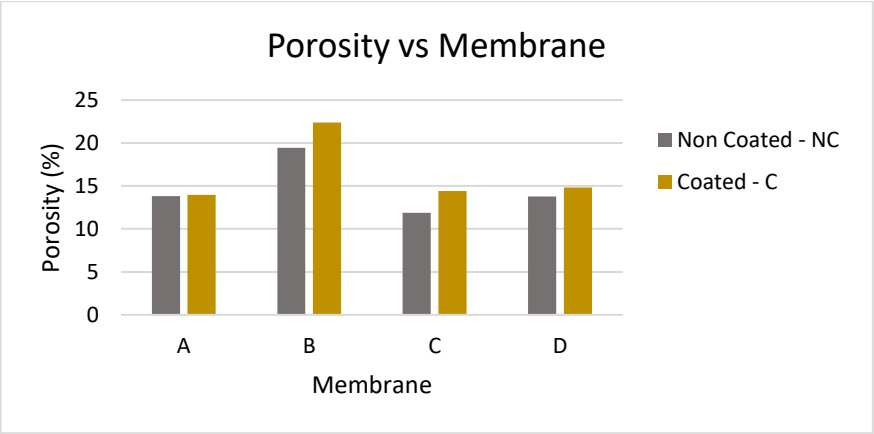

A – Laser Power 70Watt, Layer Thickness 0.06mm

B – Laser Power 70Watt, Layer Thickness 0.12mm

C – Laser Power 80Watt, Layer Thickness 0.06mm

D – Laser Power 80Watt, Layer Thickness 0.12mm

Figure 4.4: Graf showing the results surface roughness for non-coated and coated membrane.

The average data of mass of dry specimen m_d and mass of wet specimen m_w were used to reduce the impact of random fluctuations, systematic errors and outliers, contributing to a more precise and representative dataset for porosity characteristics.

Based on Figure 4.4 above, the 3D printed membrane with laser power 70W layer thickness 0.12mm for coated exhibits the highest or optimum porosity among the samples which mean hydrophobicity surface increased (Yuan et al. 2017). The optimum porosity on the bottom membrane was suitable to create hydrophobicity nature. Referring to SEM result of specimen with laser power 70W layer thickness and 0.12mm, the sizing of pore at the bottom was bigger than other membranes. The high roughness surface contains higher porosity due to the pore exhibit during printing. When a drop of water fell on this roughness surface, air was trapped in the surface cavities, creating a macroscale solid-water-air interface and an improved water contact angle.

The 80W power with a 0.06mm specimens layer may offer more efficient energy distribution and material ablation, which is more melting than 70W. When laser power is high, it will be denser, resulting in a more compact and less porous structure compared to other configurations. However, in this study, we do not want high pores and low pores. But we would like to get optimum condition of porosity to ensure the hydrophobic nature was exhibits by the membrane.

As observed, when using the same laser power, a greater layer thickness leads to an increased occurrence of pores compared to a thinner layer thickness. This is because when using a small layer thickness, there will be a lot of powder melting compared to a higher layer thickness. The reason for the occurrence of pores is because SLS printing will cause incomplete powder coalescence.

Lastly, coated membranes have higher porosity compared to non-coated membranes because candle soot that coating to the membrane is hydrophobic. The presence of a coating, especially one with irregularities like candle soot, can impact the laser-material interaction. The coating may introduce variations in energy absorption, potentially leading to uneven material processing and increased porosity. However, non-coated membranes may experience more uniform energy absorption and distribution during laser processing, potentially leading to lower porosity compared to candle soot coated.

CHAPTER 5

CONCLUSION AND RECOMENDATIONS

5.1 Conclusions

In conclusion, this project aimed to characterize the wettability of 3D printed polymer membranes for oil-water separation and determine the effect of the 3D printing process on membrane wettability. The results obtained from surface roughness, contact angle, surface morphology and porosity tests provide valuable insights into between printing parameters, material characteristics and the resulting membrane properties.

The application of candle soot coating increases water contact angle and membrane hydrophobicity, approaching superhydrophobic behaviour. Combining functional candle soot particles with various parameters in 3D printed polymer membranes proves to be an effective method for producing membranes with superior separation performance. This study highlights differences in roughness between the top and bottom surfaces of 3D printed polymer membranes, impacting distinct wettability behaviours. Higher surface roughness leads to increased water contact angles, indicating lower wettability and showcasing a superhydrophobic surface.

In conclusion, fresh 3D printed specimen with specific parameter and coating are important factors that can affect the wettability behaviour of 3D printed polymer membranes.

5.2 Recommendations for Future Study

1) Underwater Contact Angle Measurement:

It is advisable to conduct underwater contact angle assessments using an inverted sessile drop experiment setup to understand underwater wettability behaviour.

2) Soot Collection Procedure:

To guarantee precise and reliable experimental results, careful attention to experimental procedures during candle soot collection is essential. Cleaning the aluminium metal with clean water before soot collection is recommended to eliminate potential impurities that might impact coating quality.

3) Safety Measures during Sonication:

Adhering to proper protocols and safety measures, such as wearing masks and laboratory gloves during the sonication process involving hexane liquid, is crucial. This ensures a safe working environment and minimizes potential errors.

4) Comparative Analysis in Future Studies:

Future studies should include a comparative analysis of obtained results with prior research findings. This validates coating effectiveness and provides insights into performance relative to other studies, contributing to a comprehensive understanding of coating materials for practical applications.

5) Weighing Procedures for Accuracy:

Ensuring accurate measurements requires maintaining proper weighing procedures. This involves confirming that all doors on the weighing balance are closed during the

weighing process. This precaution prevents erroneous weight readings and preserves the integrity of the experimental data.

REFERENCES

Barambu, N.U. *et al.* (2021) 'Development of membrane material for oily wastewater treatment: A review', *Ain Shams Engineering Journal*. Ain Shams University, pp. 1361–1374. Available at: https://doi.org/10.1016/j.asej.2020.08.027.

Barrios, J.M. and Romero, P.E. (2019) 'Improvement of surface roughness and hydrophobicity in PETG parts manufactured via fused deposition modeling (FDM): An application in 3D printed self-cleaning parts', *Materials*, 12(15). Available at: https://doi.org/10.3390/ma12152499.

Bhushan, B. (2019) 'Bioinspired oil-water separation approaches for oil spill clean-up and water purification', *Philosophical Transactions of the Royal Society A: Mathematical, Physical and Engineering Sciences*. Royal Society Publishing. Available at: https://doi.org/10.1098/rsta.2019.0120.

Cantonati, M. *et al.* (2020) 'Characteristics, main impacts and stewardship of natural and artificial freshwater environments: Consequences for biodiversity conservation', *Water (Switzerland)*. MDPI AG. Available at: https://doi.org/10.3390/w12010260.

Chen, B. *et al.* (2022) 'Efficient oil–water separation coating with robust superhydrophobicity and high transparency', *Scientific Reports*, 12(1). Available at: https://doi.org/10.1038/s41598-022-06220-9.

Dhaka, A. and Chattopadhyay, P. (2021) 'A review on physical remediation techniques for treatment of marine oil spills', *Journal of Environmental Management*. Academic Press. Available at: https://doi.org/10.1016/j.jenvman.2021.112428.

Duman, O., Diker, C.Ö. and Tunç, S. (2021) 'Development of highly hydrophobic and superoleophilic fluoro organothiol-coated carbonized melamine sponge/rGO composite absorbent material for the efficient and selective absorption of oily substances from aqueous environments', *Journal of Environmental Chemical Engineering*, 9(2). Available at: https://doi.org/10.1016/j.jece.2021.105093.

Ezugbe, E.O. and Rathilal, S. (2020) 'Membrane technologies in wastewater treatment: A review', *Membranes*. MDPI AG. Available at: https://doi.org/10.3390/membranes10050089.

George, J.K. and Verma, N. (2022) 'Super-hydrophobic/super-oleophilic carbon nanofiber-embedded resorcinol-formaldehyde composite membrane for effective separation of water-in-oil emulsion', *Journal of Membrane Science*, 654. Available at: https://doi.org/10.1016/j.memsci.2022.120538.

Golhin, A.P. *et al.* (2023) 'Surface roughness of as-printed polymers: a comprehensive review', *International Journal of Advanced Manufacturing Technology*. Springer Science and Business Media Deutschland GmbH, pp. 987–1043. Available at: https://doi.org/10.1007/s00170-023-11566-z.

Hussein, H.A., Wais, S.I. and Khedir, K.R. (2022) 'Superhydrophobic Candle Soot Coating Directly Deposited on Aluminum Substrate with Enhanced Robustness', *Coatings*, 12(2). Available at: https://doi.org/10.3390/coatings12020202.

Hwa, L.C. *et al.* (2018) 'Integration and fabrication of the cheap ceramic membrane through 3D printing technology', *Materials Today Communications*, 15, pp. 134–142. Available at: https://doi.org/10.1016/j.mtcomm.2018.02.029.

Jung, Y.C. and Bhushan, B. (2009) 'Wetting behavior of water and oil droplets in three-phase interfaces for hydrophobicity/philicity and oleophobicity/philicity', *Langmuir*, 25(24), pp. 14165–14173. Available at: https://doi.org/10.1021/la901906h.

Kim, K.Y., Srivastava, R.P. and Khang, D.Y. (2022) 'Oleophilic to oleophobic wettability switching of isoporous through-hole membranes by surface structure control for low-voltage electrowetting-based oil-water separation', *Journal of Membrane Science*, 646. Available at: https://doi.org/10.1016/j.memsci.2022.120281.

Lazarenko, N.S. *et al.* (2022) 'Recent Advances on Membranes for Water Purification Based on Carbon Nanomaterials', *Membranes*. MDPI. Available at: https://doi.org/10.3390/membranes12100915.

Low, Z.X. *et al.* (2017) 'Perspective on 3D printing of separation membranes and comparison to related unconventional fabrication techniques', *Journal of Membrane Science*. Elsevier B.V., pp. 596–613. Available at: https://doi.org/10.1016/j.memsci.2016.10.006.

Motta, F.L., Stoyanov, S.R. and Soares, J.B.P. (2018) 'Application of solidifiers for oil spill containment: A review', *Chemosphere*. Elsevier Ltd, pp. 837–846. Available at: https://doi.org/10.1016/j.chemosphere.2017.11.103.

Mulay, M.R. *et al.* (2019) 'Candle soot: Journey from a pollutant to a functional material', *Carbon*. Elsevier Ltd, pp. 684–712. Available at: https://doi.org/10.1016/j.carbon.2018.12.083.

Pete, A.J., Bharti, B. and Benton, M.G. (2021) 'Nano-enhanced Bioremediation for Oil Spills: A Review', *ACS ES&T Engineering*, 1(6), pp. 928–946. Available at: https://doi.org/10.1021/acsestengg.0c00217.

Petzold, S. *et al.* (2019) 'Surface roughness of polyamide 12 parts manufactured using selective laser sintering', *Polymer Testing*, 80. Available at: https://doi.org/10.1016/j.polymertesting.2019.106094.

Rasouli, S. *et al.* (2021) 'Superhydrophobic and superoleophilic membranes for oil-water separation application: A comprehensive review', *Materials and Design*. Elsevier Ltd. Available at: https://doi.org/10.1016/j.matdes.2021.109599.

Rbihi, S. *et al.* (2020) 'Contact Angle Measurements of Cellulose based Thin Film composites: wettability, surface free energy and surface hardness', *Surfaces and Interfaces*, 21. Available at: https://doi.org/10.1016/j.surfin.2020.100708.

Sakthivel, S. (2021) 'Wettability Alteration of Carbonate Reservoirs Using Imidazolium-Based Ionic Liquids', *ACS Omega*, 6(45), pp. 30315–30326. Available at: https://doi.org/10.1021/acsomega.1c02813.

Sarkar, S. *et al.* (2023) 'A new methodology for measuring solid/liquid interfacial energy', *Journal of Colloid and Interface Science*, 633, pp. 800–807. Available at: https://doi.org/10.1016/j.jcis.2022.10.101.

Sutrisna, P.D. *et al.* (2022) 'Membrane fouling and fouling mitigation in oil–water separation: A review', *Journal of Environmental Chemical Engineering*. Elsevier Ltd. Available at: https://doi.org/10.1016/j.jece.2022.107532.

Wolok, E. *et al.* (2020) 'Study of bio-materials for removal of the oil spill', *Arabian Journal of Geosciences*. Springer Science and Business Media Deutschland GmbH. Available at: https://doi.org/10.1007/s12517-020-06244-3.

Xiao, Y. *et al.* (2022) 'Droplet and bubble wetting behaviors: The roles of surface wettability and roughness', *Colloids and Surfaces A: Physicochemical and Engineering Aspects*, 653. Available at: https://doi.org/10.1016/j.colsurfa.2022.130008.

Xu, H. *et al.* (2021) 'Three-dimensional structure design of tubular polyvinyl chloride hybrid nanofiber membranes for water-in-oil emulsion separation', *Journal of Membrane Science*, 620. Available at: https://doi.org/10.1016/j.memsci.2020.118905.

Yanar, N. *et al.* (2020) 'A New era of water treatment technologies: 3D printing for membranes', *Journal of Industrial and Engineering Chemistry*. Korean Society of Industrial Engineering Chemistry, pp. 1–14. Available at: https://doi.org/10.1016/j.jiec.2020.07.043.

Yuan, S. *et al.* (2017) 'Super-hydrophobic 3D printed polysulfone membranes with a switchable wettability by self-assembled candle soot for efficient gravity-driven oil-water separation', *Journal of Materials Chemistry A*, 5(48), pp. 25401–25409. Available at: https://doi.org/10.1039/c7ta08836a.

Yuan, S. *et al.* (2020) '3D printed chemically and mechanically robust membrane by selective laser sintering for separation of oil-water and immiscible organic mixtures', *Chemical Engineering Journal*, 385. Available at: https://doi.org/10.1016/j.cej.2019.123816.

UNIVERSITI TEKNIKAL MALAYSIA MELAKA
FAKULTI TEKNOLOGI DAN KEJUTERAAN MEKANIKAL

BORANG PENGESAHAN STATUS LAPORAN

PROJEK SARJANA MUDA II

Tajuk Projek : WETTABILITY BEHAVIOUR OF 3D PRINTED MEMBRANE FOR OIL REMEDIATION

Sesi Pengajian : Session 2023/2024

Saya Khairul Syazwan Naim Bin Mohd Rapi mengaku membenarkan laporan Projek Sarjana Muda ini disimpan di Perpustakaan Laman Hikmah dengan syarat-syarat kegunaan seperti berikut:

1. Laporan adalah hakmilik Universiti Teknikal Malaysia Melaka.
2. Perpustakaan dibenarkan membuat salinan untuk tujuan pengajian sahaja.
3. Perpustakaan dibenarkan membuat salinan laporan ini sebagai bahan pertukaran antara institusi pengajian tinggi.
4. Sila tandakan (✓):

☐	**SULIT***	(Mengandungi maklumat yang berdarjah keselamatan atau kepentingan Malaysia seperti yang termaktub di dalam AKTA RAHSIA RASMI 1972).
☐	**TERHAD***	(Mengandungi maklumat terhad yang telah ditentukan oleh organisasi/badan di mana penyelidikan dijalankan)
/	**TIDAK TERHAD**	

Disahkan oleh:

(TANDATANGAN PENULIS)

(COP DAN TANDATANGAN PENYELIA)

Alamat Tetap:
Lot 7058, Kampung Sura Tengah,
23000, Dungun, Terengganu

Tarikh: 27/1/2024

Tarikh:

*CATATAN: Jika laporan ini SULIT atau TERHAD, sila lampirkan surat daripada pihak berkuasa/organisasi berkenaan dengan menyatakan sekali tempoh laporan ini perlu dikelaskan sebagai SULIT atau TERHAD.